NASA

Technical Memorandum **80333**

Interplanetary Particles and Fields, November 22 - December 6, 1977: Helios, Voyager, and Imp Observations between 0.6AU and 1.6AU

L. Burlaga, R. Lepping, R. Weber, T. Armstrong, C.Goodrich, J. Sullivan, D. Gurnett, P. Kellogg, E. Keppler, F. Mariani, F. Neubauer, and R. Schwenn

AUGUST 1979

National Aeronautics and Space Administration

Goddard Space Flight Center
Greenbelt, Maryland 20771

INTERPLANETARY PARTICLES AND FIELDS, NOVEMBER 22 - DECEMBER 6, 1977: HELIOS, VOYAGER, AND IMP OBSERVATIONS BETWEEN 0.6 AU AND 1.6 AU

by

L. Burlaga
R. Lepping
R. Weber
NASA/Goddard Space Flight Center
Laboratory for Extraterrestrial Physics
Greenbelt, MD 20771

T. Armstrong
University of Kansas
Dept. of Physics
Lawrence, KS 66044

C. Goodrich
J. Sullivan
Massachusetts Institute of Technology
Cambridge, MA 02139

D. Gurnett
University of Iowa
Dept. of Physics & Astronomy
Iowa City, IA 52242

P. Kellogg
University of Minnesota
Dept. of Physics
Minneapolis, MN 55455

E. Keppler
Max-Planck-Institut fur Aeronomie
Lindau/Harz
FEDERAL REPUBLIC OF GERMANY

F. Mariani
Istituto Fisica G. Marconi
Citta Universita
Rome, ITALY

F. Neubauer
Institut fur Geophysik der I. U.
3300 Braunschweig, Mendelssohnstr. 1A
FEDERAL REPUBLIC OF GERMANY

H. Rosenbauer
R. Schwenn
Max-Planck-Institut fur Aeronomie
Katlenburg-Lindau 3
FEDERAL REPUBLIC OF GERMANY

TO BE SUBMITTED TO: Journal of Geophysical Research

ABSTRACT

In the period November 22 - December 6, 1977, three types of interplanetary flows were observed--a corotating stream, a flare-associated shock wave, and a piston-driven shock wave. Helios-2, IMP-7, 8, and Voyager-1, 2 were nearly radially aligned at $\lesssim$ 0.6 AU, 1 AU and 1.6 AU, respectively), while Helios-1 was at $\lesssim$ 0.6 AU and 35° E of Helios-2. The instruments on these spacecraft provided an exceptionally complete description of the particles and fields associated with the three flows and corresponding solar events. Analysis of these data revealed the following results. 1) A coronal hole associated corotating stream, observed at 0.6 AU and 1 AU, destroyed itself before it reached 1.6 AU. The stream interface corotated and persisted with little change in structure even though the stream disappeared. A forward shock was observed ahead of the interface, and moved from Helios-2 at 0.6 AU to Voyager-1, 2, at 1.6 AU; although the shock was ahead of a corotating stream and interface, the shock was not corotating, because it was not seen at Helios-1, probably because the corotating stream was not stationary. 2) An exceptionally intense type III burst was observed in association with a 2B flare of November 22. The exciter of this burst--(a beam of energetic electrons)--and plasma oscillations (presumably caused by the electron beam) were observed by Helios-2. 3) A non-spherical shock was observed in association with the November 22, flare. This shock interacted with another shock between 0.6 AU and 1 AU, and they coalesced to form a single shock that was identified at 1 AU and at 1.6 AU. 4) A shock driven by a piston was studied. In the piston, the density and temperature were usually low and the magnetic field intensity was relatively high. This region was preceded by a directional discontinuity at which the magnetic field intensity dropped appreciably. The shock appeared to move globally at a uniform speed, but locally there were fluctuations in speed and direction of up to 100 km/s and 40°, respectively. 5) Three types of electrostatic waves were observed at the shocks, in different combinations. The detailed wave profiles differed greatly among the shocks, even for spacecraft separations $\lesssim$ 0.2 AU, indicating a strong dependence on local conditions. However, the same types of fluctuations were observed at 0.6 AU and at 1.6 AU. 6) Energetic (50-200 keV) protons were accelerated by

the shocks. The intensities and durations of the fluxes varied by a factor of 12 over longitudinal distances of $\lesssim$ 0.2 AU. The intensities were higher and the durations were lower at 1.6 AU than at 0.6 AU, suggesting a cumulative effect. 7) Energetic ($\lesssim$ 50 keV) protons from the November 22, flare were observed by all the spacecraft. During the decay, Helios-1 observed no change in intensity when the interface moved past the spacecraft, indicating that particles were injected and moved uniformly on both sides of the interface. Helios-2 observed an increase in flux not seen by Helios-1, reaching maximum at the time that a shock arrived at Helios-2. The intensity dropped abruptly when the interface moved past Helios-2, indicating that the "extra" particles seen by Helios-2 did not penetrate the interface.

1. INTRODUCTION

In the period November 22 to December 6, 1977 Helios-1 and -2, IMP-7 and -8, and Voyager-1 and -2 were aligned very favorably for the investigation of solar outputs (Figure 1), and during this period several significant solar events occurred. Recognizing that this interval (and a similar interval in September-October, 1977) offered a unique opportunity for a comprehensive study of interplanetary shocks, flows, magnetic fields, and energetic particle phenomena, a Workshop was organized to bring together experimenters from the Helios, Voyager and IMP programs. The meeting was organized by Dr. S. M. Krimigis, with the support of the Voyager and Helios team leaders. This paper is based on some of the results of that Workshop. The purpose of this paper is to present a description and an analysis of the principal interplanetary events that were observed in the period November 22-December 6, 1977, by Helios-1, 2, Voyager-1, 2, and IMP-7, 8.

Three flow systems were observed in the period under consideration: 1) a corotating stream and a stream interface associated with a coronal hole, 2) a shock wave an and energetic particle event associated with a 2-B flare, and 3) an isolated shock wave whose origin is uncertain.

This paper is based on data from 28 experiments from 6 spacecraft. The experiments and the corresponding principal investigators are listed in Table 1. Nearly complete measurements of solar wind plasma, magnetic fields and plasma waves are available from all spacecraft. Radio waves, plasma waves and energetic electrons associated with the November 22, event are available from Helios-1,2 and Voyager-1, 2. Data describing low energy protons associated with the November 22, event are available from Helios-1, 2 and Voyager-1, 2.

We begin in Section 2 by discussing the corotating stream and its associated shock and interface; this flow system was relatively simple, and the other two events interacted with it. Section 3 discusses the particles, fields and flows associated with the flare of November 22. Section 4 analyses a relatively simple, isolated shock wave that passed all of the spacecraft in the early days of December, 1977. Plasma waves at the shocks in the three events are discussed qualitatively in Section 5. Energetic protons accelerated by the shocks and injected by the November 22 flare are described in Section 6. Section 7 summarizes the results.

2. COROTATING STREAM, INTERFACE AND SHOCK

A stream that was observed successively by Helios-1, Helios-2, IMP-7, 8, Voyager-1 and Voyager-2 is shown in Figure 2, which shows bulk speeds from the experiment of Rosenbauer on Helios-1, 2 and from the experiments of Bridge on IMP-7, 8 and Voyager-1, 2. Sixteen minute averages of V are plotted versus time, and the phase is chosen such that the arrival time of the stream interface at each spacecraft is coincident with the vertical line marked "interface". A stream interface is a relative thin boundary that marks the transition between a quasi-stationary stream flow and the material ahead of it. It is readily identified as an abrupt decrease in density and an abrupt increase in temperature at the front of a stream (Belcher and Davis, 1971; Burlaga, 1974, 1975). In this case, the interface at each spacecraft can be seen in Figure 3, where the time profiles of 16-min averages of the density (n) and temperature (T) are plotted. Figure 2 shows that the interface and stream arrived at Helios-1 on November 23, at Helios-2 on November 25, at earth on November 27, and at Voyager-1 and -2 on November 29. The 2-day interval between successive encounters of the interface is approximately that which is expected for a "corotating spiral" corresponding to a streamline with a speed of 400 km/s, as illustrated at the bottom of Figure 2.

The precise corotation times of the interface from one spacecraft to the next are shown in Table 2, together with the "predicted" corotation times computed from the equation $t_2 - t_1 = (r_2 - r_1)/V + (\phi_2 - \phi_1)/\Omega_s$, with allowance for the spacecraft motions (here Ω_s is the sidereal rotation period of the sun; V is the solar wind speed; ϕ_1 and ϕ_2 are respectively the longitudes of the spacecraft at time t_1 (when the interface passed the first spacecraft) and a later time t_2 (when the interface passed the second spacecraft); and r_1 and r_2 are the radial distances from the sun of the two spacecraft at t_1 and t_2.) Table 2 shows that the predicted corotation times are close to the observed corotation times, the difference being $\lesssim$ 15% in the three largest time intervals. These small differences may be due to small irregularities in the shape of the surface of the interface. Thus, we conclude that the interface was a corotating feature, and we infer that the stream which followed it was likewise corotating.

The low densities in the stream (Figure 3) and the fact that it was corotating suggest that its source was a coronal hole (Hundhausen, 1977; Burlaga, 1979). A coronal hole, tentatively identified in the Kitt Peak He 10830A° maps, passed central meridian on November 24, 25. The observed peak speed of the stream in question was $\gtrsim$ 500 km/s; thus, if its source was the coronal hole, and if it propagated at nearly constant speed, the stream should have arrived at the earth on November 27, which in fact, it did.

The dynamical evolution of the corotating stream in Figure 2 is surprising and significant. Helios-1 and -2 observed similar profiles of V(t), n(t), and T(t) following the interface, with a time delay of $\gtrsim$ 53 hrs consistent with corotation. At the earth, IMP-7 and IMP-8 also saw the stream with approximately the expected corotation delay. The surprising result is that the stream appears to have been absent (or much slower) at Voyagers-1, and -2 (Figure 2), even though both spacecraft observed the stream interface (Figure 3). This is not a latitude effect like that reported by Schwenn et al., (1978), since the latitudes of Voyager-1 and Earth differed by only 1.5° (the latitude of Voyager-2 was $\simeq$ 5.2° higher than that of Earth). Thus the stream apparently destroyed itself in moving between 1 AU and 1.6 AU.

Although a numerical model is needed to show quantitatively that a stream can be dissipated near 1 AU as just described, one can understand the result qualitatively as follows. Ahead of the stream, the density and hence the momentum flux were high (Figure 3). Inside the stream the density was low and the speed of the stream itself was relatively low; hence the momentum flux of the stream did not greatly exceed that of the flow ahead of it. As the stream evolved, stress was relieved somewhat by shear at the interface. Nevertheless, two compression waves formed, moving toward and away from the sun with respect to the interface, respectively. The wave moving toward the sun (i.e., into the stream) decelerated the stream. The wave moving away from the sun (i.e., ahead of the stream) evolved into a forward shock (see below). The importance of momentum flux in corotating stream dynamics has been discussed quantitatively by Pizzo (1979a,b) for some conventinal stream profiles.

The structure of the stream interface observed by Voyagers-1 and -2 is shown in Figure 4. In both cases, the density and temperature transi-

tions occured in $\sim$ 30 min, consistent with some of the relatively thin interfaces observed at 1 AU by Burlaga (1974) and Gosling et al. (1978). (The n, T profiles observed at Helios-1, 2 are very similar to those in Figure 4.) The magnetic field intensity reached a maximum at the interface (see Figure 4), as is usually the case (Burlaga, 1974; Siscoe, 1972). In this case, there was a large change in magnetic field direction across the interface at both Voyager-1 and -2. It is significant that all of the parameters just described (n, T, V, and $\underset{\sim}{B}$) had nearly the same profile at Voyager-2 as at Voyager-1, despite the separation of $\sim$ 0.2 AU; this shows that the internal structure of a stream interface can be coherent over a relatively large distance. Plasma wave observations at the interface at Voyager-2 (Figure 4) show no significant wave emission in the frequency range 10 Hz to 562 Hz, suggesting that the interface was relatively stable. Similar observations of a different interface described by Gurnett et al. (1979a) showed the same result.

A "corotating shock" (which we label shock B) was observed by Voyagers-1 and -2; this is shown at high resolution in Figure 5. The identification of the disturbance as a shock is based on the simultaneous, abrupt increases in V, N_p, T_p and $F \equiv |\underset{\sim}{B}|$, and on the simultaneous change in the characteristics of the plasma waves. The observation of a shock at Voyager-1 and -2 is not surprising, since models of corotating streams (e.g., Hundhausen, 1973; Hundhausen and Burlaga, 1975; Gosling et al., 1976; Steinolfson et al., 1975; and Dryer et al., 1978) predict the development of corotating shocks as streams evolve with distance from the sun, and many such shocks have been observed beyond 1 AU (Smith and Wolfe, 1977). The shock normals computed from the Voyager plasma and magnetic field data using the method of Lepping and Argentiero (1971) were directed 9° and 14° west of radial, respectively (see Table 3 and Figure 2), consistent with corotation. At Voyager-2, the angle between the shock normal and the upstream magnetic field was 14.6°; the corresponding angle at Voyager -1 was 15.8°. The local shock speed was 400, $\pm$ 10 km/s relative to a fixed frame shock at both Voyager-1 and Voyager-2 (Table 3). This speed and the computed shock normals imply a time delay between Voyager-1 and Voyager-2 of 4.5 $\pm$ 1.3 hr. This compares favorably with the observed time delay of 5 hr. 17 min.

Shock B probably passed Helios-2 and IMP-8 on November 25 and 26, respectively (see Table 3). This is significant, because shocks are rarely observed ahead of corotating streams at $\lesssim$ 1 AU (Ogilvie, 1974). The identification of shock B at Helios-1 is based on the observations that 1) the magnetic field intensity measured by Neubauer's instrument increased from $\sim$ 7γ to $\sim$ 15γ within 2 minutes (it increased from 7.7γ to 11.5γ in 64s), and 2) the plasma speed density and temperature increased between 0122 and 0205 UT (see Figures 2 and 3). The shock normal computed from the magnetic field data using the coplanarity theorem, is $\lambda_n = 60°$, $\theta_n = 14°$, which is close to that expected for corotation in a 300 km/s wind, viz. $\lambda_n = 50°$, $\theta_n = 0$; here λ_n is the heliographic longitude which is taken to be zero for a vector pointing radially away from the sun, and θ_n is the latitude with respect to the ecliptic plane. The shock speed computed from the observed densities and bulk speeds using the coplanarity normal is 300 km/s, or 540 km/s in the radial direction. This implies that the shock should have arrived at earth 41 hrs after it passed Helios-2 (if it moved at constant speed), i.e., at hr 19 on November 26. A SSC was reported at 1704 UT on November 26, in good agreement with the prediction. IMP-8 was in the solar wind on November 26, but there are data gaps at the time of the SSC. Nevertheless, the magnetic field intensity nearly doubled at some time in a 2-hr interval centered about the SSC (Figure 3), and the plasma density, temperature and speed increased at some time in a 5-hr data gap which included the time of the SSC (Figures 2 and 3). Thus, the IMP-8 data are consistent with the presence of a shock at Earth at 1704 on November 26. Altogether, the data from Helios-2, IMP-8 and the SSC give fairly convincing evidence for a shock driven by a corotating stream, which moved nearly radially from 0.6 AU to 1 AU and on to Voyager-1, 2 at 1.6 AU. Figure 3 shows that the shock moved away from the interface during the time that it moved from 0.6 AU to 1.6 AU.

It is customary to refer to a shock ahead of a corotating stream as a corotating shock. This is not appropriate for shock B, however. If shock B were corotating, then it should have been detected at Helios-1 $\sim$ 50-60 hr before it was observed at Helios-2 (i.e., late on November 23), because Helios-1 was at the same radial distance as Helios-2 and $\sim$ 35° to the East. Although the Helios-1 observations are nearly complete and continuous, there is no evidence of a shock at Helios-1 (see Figures 2 and 3). A

possible explanation is that the stream which produced the shock was corotating but not stationary. For example, the stream may have been produced by a coronal hole that rotated with the sun, but whose physical characteristics changed on a scale of 1 day, producing a time-varying stream profile. Indeed, Figure 2 shows that the speed profile measured by Helios-2 differs in some details from that measured by Helios-1, indicating some time variations in this case. Evidence for non-stationary, corotating streams was presented earlier by Burlaga et al. (1978). Shock B was seen at Helios-2, IMP-8, and Voyager-1, 2 because those spacecraft were near a radial line; once formed at $\leq$ 0.6 AU the shock persisted and was convected past the other spacecraft. But apparently conditions were different at the time the stream was at Helios-1, 35° E of Helios-2, and were not favorable for the production of a shock.

3. EVENTS ASSOCIATED WITH A FLARE

On November 22, 1977 at 2B flare at N23, W40 in McMath plage region 15031 was observed in H_α starting at 0946 UT and reaching maximum intensity at 1006 UT. Chambon et al. (1978) observed hard X-rays and γ rays from the flare starting at $\sim$ 1000 UT. It produced a SID, a type IV burst (starting at 1002), a type III burst (beginning at 0959 UT), an interplanetary shock wave, and an energetic particle event. Thus, the event displayed a wide range of phenomena that one associates with a great flare (Dryer, 1974).

Type III Bursts. The type III solar radio burst produced by the flare is the most intense observed to date by Helios-1 and -2. Helios-2 radio observations of the November 22 burst are shown in Figure 6. They are from the University of Minnesota (52, 77 and 203 kHz) and Goddard Space Flight Center experiments. Electron observations from the Max-Planck-Institute fur Aeronomie experiment are also displayed in Figure 6, showing that electrons in and near the 20-65 keV energy range were present, consistent with the idea that low frequency type III solar radio emission is caused by electrons with energies 10 keV to 100 keV (Lin et al., 1973). Despite the data gap around 1010 UT, it is clear that the radio burst was double-peaked at the higher frequencies, possibly due to two separate bursts; however there was only a single peak at lower frequencies. The first peak reached maximum intensity at 1001 UT for 3 MHz, and the merged peak is observed at 1032 UT for 77 kHz. Much of this delay corresponds to the transit time for

the energetic electrons from a heliocentric distance of 0.05 AU (3 MHz level) out to 0.8 AU (77 kHz level), indicating an outward speed greater than 0.2c for the exciter. A few minutes of the delay arise from the difference in propagation time of the electromagnetic waves from the source levels to Helios-2, located at 0.6 AU.

Flux densities observed for this burst by Helios-2 reached maximum values exceeding 10^{-15} $Wm^{-2}Hz^{-1}$ for frequencies from 77 to 255 kHz; they decreased to approximately 10^{-16} $Wm^{-2}Hz^{-1}$ at 3 MHz, the highest Helios observing frequency. The 52 kHz channel, which shows strong electrostatic noise from 1025 to 1050 UT, is at the peak of the electrostatic noise spectrum, and it is within 1-2 kHz of the local plasma frequency determined from the measured density. Similar bursts were reported by Gurnett et al. (1978) and Gurnett and Anderson (1977). The electrostatic bursts might be short compared to the sampling time of the tuned receiver. The bandwidth of the receiver is about 5 kHz and its rise time, therefore, is about 0.2 msec, which is instantaneous compared to the detector integration time to 50 msec. As a consequence, for signals whose duration is more than 0.2 msec, the measurement gives the input voltage averaged over 50 msec.

The 77 kHz channel is the lowest frequency which did not show electrostatic noise. Burst radio emission has been reported to be generated at twice the local plasma frequency (Alvarez et al., 1972). Consequently the 77 kHz electromagnetic waves detected at 0.60 AU by Helios-2 were propagating backward toward the sun from a source level near 0.8 AU, where the plasma frequency is half of 77 kHz.

This burst and the associated electron beam were also observed by the Voyager-1 and -2 planetary radio astronomy experiment and low energy particle experiment, respectively. The burst arrival directions, found by the spinning Helios-1 and -2 antennas, together with the Helios and Voyager electron data, show that the exciter extends over a wide (> 75°) range of solar longitudes. Analysis of the relative intensities and positions observed by Helios-1 and -2 also indicates that the centroid of the burst passed between these two spacecraft. Assuming a source longitude of 40° W and a spiral field configuration, a best fit to the intensity versus frequency data obtained by Helios-1 and -2 is obtained for a solar wind speed of 300 km/sec. This is consistent with the speeds measured by the Helios plasma instruments, which were near 300 km/sec for several days.

Interplanetary Shocks and Flows. The interplanetary shock wave produced by the flare was observed directly by Helios-1 and -2, IMP-8, and Voyager-1 and -2; it was also observed indirectly as a SSC at the earth (see Table 4 and Figure 7). The snock might have been driven by a piston, as suggested by the sketch in Figure 8, but the piston was not actually observed, because no spacecraft was suitably positioned.

If one tries to determine the motion of the shock using a radial distance vs. time plot (Figure 9) and the customary assumption of spherical symmetry, he encounters difficulties that would have been overlooked if there were fewer spacecraft. One difficulty is that the speed determined from the time delay between IMP-8 and Voyager-1 is 418 km, whereas the speed determined from the time delay between IMP-8 and Voyager-2 is 568 $\pm$ 20 km/s (the uncertainty is due to a data gap at Voyager-2 between 06:00 and 09:00 UT). This discrepancy is large, considering that Voyager-1 and Voyager -2 were separated by only 0.005 AU in the radial direction and by 0.2 AU in the transverse direction.

A second and more extreme example of the inadequacy of the assumption of spherical symmetry for computing shock speeds is the speed determined from the time delay between Voyager-1 and Voyager-2: 14 $\pm$ 2 km/s! This is obviously wrong, and it is far from the speed determined from the analysis of the shock data at Voyager-1 (Figure 10), viz. 302 km/s. The shock normal and speed computed from the Voyager-1 data using the method of Lepping and Argentiero (1971), were (λ_n = -34°, θ_n = -10°) and V_n = 302 km/s, respectively (see Table 4). Using these numbers, assuming that the shock was plane between Voyager-1 and Voyager-2, and considering the inertial solar ecliptic positions of Voyager-1 (r_1 = (2.280, -0.274, 0.115) x 10^8km) and Voyager-2 (r_2 = 2.285, -0.533, 0.267) x 10^8km), one finds that the predicted time delay between Voyager-1 and Voyager-2 is 11 hrs, 13 min, which is reasonably close to the observed delay, (15 $\pm$ 1.5) hrs. (The $\pm$ 1.5 hr uncertainty is due to a data gap.) The small discrepancy may be attributed to uncertainties in the shock normal and to curvature of the shock surface. By contrast, the time delay predicted using the assumption of spherical symmetry is only 36 min. We conclude that the use of time delays and assumption of spherical symmetry does not always give accurate shock speeds, whereas the use of local jump conditions and observations did give reasonably accurate estimates of the shock speed and direction in this

case. The observed orientation of the shock is consistent with that expected for a shock with a radius of curvature less than 1.6 AU, originating at the flare site.

Helios-2 observed two shocks (A_1 and A_2, at 1610 UT on November 23 and at 0611 UT on November 24, respectively; see Figures 7 and 11). However IMP-8, which was at nearly the same latitude and longitude and which was only 0.36 AU away from Helios-2, observed only one shock (A_4 at 1213 UT on November 25; see Figures 7 and 10). We cannot unambiguously determine why 2 shocks passed Helios-2 (several origins can be imagined), but we can suggest why only one shock was subsequently observed at IMP-8 and at Voyagers-1 and -2. The radial speed of shock A1, determined from the local plasma and magnetic field observations of the shock by Method MD1 of Abraham-Shrauner and Yun (1976), was 353 km/s. The corresponding speed of A_2 was 467 km/s. Thus, although A_2 followed A_1 (i.e., it was closer to the sun, see Figure 7), it was moving faster than A_1. Consequently, A_2 should have overtaken A_1 at some point; assuming constant speeds, this point was at 1.08 AU on the Helios-2-sun line. If the computed shock normals (Table 4 and Figure 7) are even approximately correct, the shocks should have interacted along the earth-sun line before they reached IMP-8 near the earth. The observation of only one shock at IMP-8 suggests that when the shocks interacted, they coalesced. This is in agreement with gas dynamic theory where the overtaking of one shock ($\overline{A_1}$) by a following one (A_2) leads to a coalesced shock moving forward and a reverse rarefaction fan which, because of its spreading, is difficult to observe. (In MHD the interaction leads to seven distinct MHD-structures the most prominent ones of which are a forward fast shock and a reverse fast rarefaction wave.) The resultant shock propagated to Voyager-1, which was close to the earth-sun line. Its radial speed at V1, determined from the shock observations using the method of Lepping and Argentiero (1971), was 369 km/s, which is in reasonable agreement (considering typical normal errors) with the speed determined from the time delay between IMP-8 and Voyager-1, viz 427 km/s. Evidence for shock-coalescence in Pioneer data has been reported by Smith *et al.* (1977). A second alternative would be a sufficient weakening of one shock before it interacted with the other one. Note that the very weak shock would still have to interact with the second shock. This possibility is ruled out by the following two arguments: A_2 cannot be the weakened shock

since it fits very nicely into the propagation diagram (Figure 9) in contrast to shock A_1. We rule out a large weakening of shock A_1 since it is followed by a long-lasting region of increased momentum and energy flux as shown in Figure 7.

A remaining aspect which requires clarification is the observation of one shock only at Helios-1. A possible explanation for this observation may be the presence of the stream interface and an interaction region between Helios-1 and Helios-2 (Burlaga and Scudder, 1975). If we approximate it as a tangential discontinuity, it may lead to the complete disappearance of one shock (see e.g., Neubauer, 1976).

4. THE DECEMBER SHOCK

During the Helios-Voyager-IMP Workshop, it was noted that a shock was observed by Helios-1 and -2 on December 1 and by Voyagers-1 and -2 on December 2, and it was decided to include this event in the joint study. The interplanetary data are nearly complete, as shown in Figure 12. However, the solar data do not show any large flare which might have produced the shock. One candidate is an SN flare at S24, E85 which began in H_α at 0338 UT on November 30 and reached a maximum at 0350 UT. This small flare was associated with an X-ray burst (starting at 0330 UT, with a maximum at 0348 UT) and a SID (starting at 0334 UT, with a maximum at 0349 UT). In view of the uncertainty concerning the source of the shock, our discussion emphasizes the interplanetary observations.

Post-shock conditions. The density and temperature profiles in Figure 12 suggest that the shock observed by Helios-1 was followed by a piston in which the density and temperature were low. There is also evidence for enhanced magnetic field intensities in the piston. Helios-2 may also have observed the piston (Figure 13), but this is less certain because of a data gap. The shock was also detected by Voyager-1 and -2 (See Figures 13 and 14), but they did not encounter the piston. Thus, the evidence is that the shock had a wide longitudinal extent ($\gtrsim 40°$; see Figure 15), and was driven by a piston less broad, originating east of the Voyager-Sun line.

Note that Voyager-1 and -2 observed a monotonic decrease in speed, density, temperature, and magnetic field intensity behind the shock (Figure 13). Many authors have interpreted such a signature as evidence for a blast wave, generally on the basis of observations from just one

satellite. However, observations of a piston at Helios-1 indicate that this was probably not a blast wave; it was a driven shock. Voyager-1 and -2 saw the shock, but they did not encounter the piston due to the piston's more limited longitudinal extent. This shows that the signature of the post-shock flow is not sufficient to identify the type of a shock wave. This point was made previously by Ogilvie and Burlaga (1974), and it has recently been demonstrated very clearly by Acuna et al. (1979). The concept of a broad shock driven by a narrow piston is not new, although it is often forgotten or ignored. It dates back at least to Gold (1959).

Shock motion. Figure 16 gives a plot of radial distance versus time, showing the shock positions and times determined from the observations of Helios-1, -2, Voyager-1, -2 and from a sudden commencement at Earth. The points lie very close to a straight line with a slope corresponding to a speed of 555 km/s. Considering that Helios-1 was 19° east of the Voyager-2-sun line and that Earth was 17° west of that line, the straight line in Figure 16 suggests a nearly spherical shock front moving at a constant speed between 0.6 AU and 1.6 AU. Similar results for the August, 1972, events were reported by Smith et al. (1977) and Dryer et al. (1976). However, examination of the local shock speeds and normals reveals a more complicated picture. Since Voyager-2 and Helios-2 were nearly radially aligned, and since Figure 16 suggests a spherical shock, one expects that Voyager-2 and Helios-2 should have observed essentially the same shock speed and direction, the radial component of velocity being close to 555 km/s. The local jump conditions give rather different results (Table 5): 1) The local speeds were substantially less than the speed determined from the average speed determined from the time delay; and 2) the shock normal at Helios-2 ($\lambda_n = -3°$, $\theta_n = 17°$) was very different from that at Voyager-2 ($\lambda_n = 38°$, $\theta_n = -6°$). These differences are too large to be attributed to uncertainties in the computation of the local shock speed and direction. The field and plasma parameters were relatively steady before and after the shock, the field direction change was relatively large (18° at Helios-2), and we used both magnetic field and plasma observations; so we expect the uncertainty in speed to be $\lesssim$ 20 km/s and the uncertainty in direction to be $\lesssim$ 10° (Abraham-Shrauner and Yun, 1976; Lepping and Argentiero, 1971). Thus the observations suggest that locally the shock surface may have been distorted such that the normal was not radial, although the normal may have

been radial on average. Likewise, locally the shock may have been accelerated or decelerated giving local speeds higher than average in one place, lower than average in a second place, and near-average in a third place (Heineman and Siscoe, 1974; Burlaga and Scudder, 1975). For example, the radial component of the local velocity at Voyager-2 (530 km/s) is consistent with the average speed determined from time delay (555 km/s) within the experimental uncertainties, but the radial component of the local velocity at Helios-2 (460 km/s) is substantially less than the average value. We conclude that the radial component of the shock velocity may have fluctuated as much as $\approx \pm$ 100 km/s, and its direction may have fluctuated as much as $\pm$ 40° as it moved between 0.6 AU and 1.6 AU.

5. PLASMA WAVES AT SHOCKS

Helios-1, -2 and Voyager-1, -2 carried plasma wave instruments (see Gurnett and Anderson, 1977; and Scarf and Gurnett, 1977, respectively for a discussion of the instruments), which provided an extensive set of observations of waves near the interplanetary shocks discussed above. These observations were used as a means of searching for and confirming the identity of the shocks. More important, however, they provide an exceptionally large and complete record which form a basis for a comparative study of waves at interplanetary shocks. Only a few papers discussing plasma wave electric fields at interplanetary shocks have been published (Scarf, 1978; Scarf *et al.*, 1979, and Gurnett *et al.*, 1979a,b). Here we shall present only a qualitative discussion stressing the remarkable variety of signatures. A more comprehensive physical discussion is deferred to another paper.

The wave data are given together with the plasma and magnetic field observations of the shocks in Figures 5, 10, 11, 12, and 14. The electric field intensity is plotted versus time for each of several frequency channels on a logarithmic scale with a range of 100 db for each channel. The electric field strength ranges from about 1μ V m^{-1} at the bottom of the scale to 100 mV m^{-1} at the top of the scale. The solid lines represent peak electric field amplitudes and solid black areas (or vertical solid lines in some cases) represent the average electric field amplitude.

Let us consider the individual shock observations in the order in which shocks were introduced above, beginning with shock B. This shock had not

developed at the position of Helios-1, but it was observed at both Voyager-1 and Voyager-2 (Figure 5), which were at essentially the same radial distance (1.6 AU) and separated by $\lesssim$ 0.2 AU. The Voyager-1 plasma wave observations show at least three different types of emissions:

1. turbulence extending downstream of the shock at frequencies $\lesssim f_p^+$, identified as whistler mode turbulence
2. waves extending upstream at frequencies from about 1.0 to 5.62 kHz, tentatively identified as ion acoustic waves, and
3. a short, well-defined broadband burst at the shock at frequencies from 10 Hz to 5.62 kHz.

These types of emissions have been discussed by Scarf et al. (1970), Gurnett and Frank (1978), and Gurnett et al. (1979b). Voyager-2 also observed the whistler mode turbulence extending downstream from the shock, and it observed a peak corresponding to the broadband emissions at the shock. There are no Voyager-2 data above 1 kHz, probably due to a failure in the spacecraft data system which reduced the sensitivity of these channels.

Plasma waves at shock A were observed by Helios-2 (Figure 11), and by IMP-8 and Voyager-1 (Figure 10). Whistler waves were not observed downstream of the shock at Helios-2 and IMP-8, but they were observed downstream of the shock at Voyager-1. The shock at Helios-2 is almost totally obscured by a broad region of ion acoustic wave turbulence from about 562 Hz to 10 kHz; these waves are not necessarily all associated with the shock (Gurnett and Frank, 1978). IMP-8 and Voyager-1 observed ion acoustic waves upstream of the shock between f_p^+ and f_p^-. Helios-2 observed a sharp burst of noise in the 311 and 562 Hz channels coincident with the passage of shock; IMP-8 found some evidence of a corresponding noise burst below f_p^+, and Voyager-1 observed a noise burst at the shock in the range 31 Hz to $\lesssim$ 1.78 kHz.

Shock C was observed by Helios-1 and -2 and by Voyager-2 (Figures 12, 13, and 14). None of the spacecraft observed intense whistler mode turbulence behind the shock. Helios-1 and Helios-2 observed an enhancement in electric field intensity in the range 562 Hz to 10 kHz with a large peak to average ratio, probably due to Doppler-shifted ion-acoustic waves (Gurnett and Frank, 1978). The waves extended both upstream and downstream

at Helios-1, but only downstream at Helios-2. Voyager saw only weak emission of such waves, downstream of the shock: A sharp, intense (1 to 5 mV m^{-1}) broadband burst of electric field turbulence was observed at Helios-2, but it was absent at Voyager-2 and missing or obscured by the ion acoustic waves at Helios-1.

We conclude that at least three types of emissions (in various combinations) may be observed at an interplanetary shock, viz., downstream "whistler-mode turbulence", upstream "ion-acoustic" waves, and a brief broadband noise burst coincident with the shock. In some cases, only one or two of these is observed. In addition, the shock may be embedded in a broad region of "ion-acoustic" waves not necessarily caused by the shock. The combination of wave-types and the characteristics of each wave mode seen at one spacecraft may be very different from those observed by another spacecraft nearby. Apparently, the plasma waves at a shock depend strongly on the local characteristics of the medium. However, the basic types of emissions are the same at 0.6 AU as they are at 1.6 AU.

6. ENERGETIC PROTONS

In the interval November 22 to December 6, 1977, Helios and Voyager instruments observed energetic protons ($\lesssim$ 50 to 200 keV) produced by at least two mechanisms: local shock acceleration and acceleration in a flare. It is convenient to begin by discussing the former, since shock accelerated particles are less complicated by propagation effects.

Shock Acceleration. Protons accelerated by a shock are seen most clearly in the case of shock C which was relatively isolated and uncomplicated, as discussed in Section 4. Recall that Voyager-1 and -2 observed a shock behind which the flow parameters and magnetic field intensity dropped gradually to the preshock values; there was no evidence of a piston at their positions. Figure 17 shows enhancements in the counting rate of protons at Voyager-1 and -2 in the energy range $\lesssim$ 50 keV to $\lesssim$ 138 keV; the maximum intensity occured at or just behind the shock. At Voyager-2 the peak counting rate was $\lesssim$ 100 times the ambient value, and at Voyager-1 the enhancement was somewhat smaller. The enhancement began $\lesssim$ 15 hr ahead of the shock at both Voyager-1 and -2. It persisted for $\lesssim$ 32 hr behind the shock at Voyager-1 and $\lesssim$ 28 hr behind the shock at Voyager-2. There were small differences in the shapes of the profiles which might be

due to differences in the local magnetic field configurations. Basically, however, the proton enhancement at Voyager-1 was similar to that at Voyager-2. This may be due to the simple geometry of the shock near Voyagers-1 and -2 and to their relatively small separation (0.2 AU).

The situation at Helios-1 and -2 was quite different. Both spacecraft observed an enhancement in counting rate of protons (Figure 17). The maximum enhancement at Helios-2 was only $\sim$ 20 times the background counting rate and it occurred at the shock. Two maxima were observed by Helios-1, and the shock occurred between them. A compression wave was observed at the time of the second maximum (Figure 12), but the time resolution was not adequate to determine whether or not it was a shock. The counting rate dropped abruptly approximately 6 hr after the shock at both Helios-1 and -2, in contrast to the more gradual, longer lasting decline at Voyagers-1 and -2. This might be due, at least in part, to the presence of a piston at Helios-1 and at Helios-2, which was not observed by Voyagers-1 and -2. (There is no accepted signature for a piston boundary, and we cannot be certain that we have identified one. The vertical line labeled "piston" in Figure 17 corresponds to an abrupt decrease in density observed behind the shocks in Figure 12 and 13). The enhancement began $\sim$ 6 hr ahead of the shock at Helios-2 and a few hours ahead of the shock at Helios-1; the slight difference could be due to different acceleration efficiencies of the two shocks and/or to different upstream magnetic field conditions which gave connection to the shocks at slightly different times. There is a curious enhancement at Helios-1, occurring several hours ahead of the shock-associated enhancement but closely resembling it. One can imagine that this was due to a magnetic field geometry which provided a good connection between the observer and the shock for several hours before the shock arrived.

The differences between the enhancements at Helios-1 and Helios-2 and the differences between the enhancements at Voyager-1 and Voyager-2 indicate that local conditions do influence the intensity profile somewhat. Note, however, that the Voyager-1, -2 profiles have a greater maximum enhancement and a greater upstream extent than the Helios-1, -2 profiles. One possible reason for this (but not the only one) is that Voyager-1, -2 were farther from the sun than Helios-1, -2, so that the shock at Voyager-1, -2 had been accelerating particles for a longer time and perhaps

accelerated and accumulated more particles than it had when it was at the positions of Helios-1 and -2.

Flare-accelerated Particles. Now let us discuss the low energy ($\lesssim$ 25 - 200 keV) protons ejected by the flare of November 22, 1977 (see Section 3 for a discussion of the flare characteristics and the corresponding interplanetary flows). Helios-1 and -2 observed very different intensity-time profiles during the decay in intensity (Figure 18), even though they were at nearly the same radial distance and were separated in longitude by only 32° (see Figures 1 and 8). At Helios-1, the intensity decreased smoothly and monotonically for at least 3 days (Figure 18). The corotating, stream discussed in Section 2 was east of Helios-1 at the beginning of the event and the interface passed the spacecraft $\lesssim$ 16 hr later with only a small perturbation on the intensity-time profile. Apparently the flare injected particles over a broad range of longitudes near the sun, so that the intensity versus longitude was nearly uniform across the corotating interface. The particles in the slow flow ahead of the interface decayed freely (e.g., by diffusing to infinity, Kurt et al., 1978) for at least 16 hrs after the flare, and the particles in the corotating stream decayed similarly for at least three days after the flare. In particular, particles in the corotating stream were unaffected by the flare associated shock wave (shock A) and the post shock flow (see Section 3 and Figure 8).

The intensity-time profile at Helios-2 was quite different from that at Helios-1, probably because it was influenced by the flare-associated shock and post-shock flow. The early part of the decay seen by Helios-2 was very similar to that observed by Helios-1 (Figure 18), the flux decreasing monotonically for at least 12 hrs. As shock A_1 (produced by the flare) approached Helios-2, the counting rate of energetic protons began to increase, reaching a maximum at the time shock A_2 reached Helios-2. The maximum flux was $4 < 10^6$ ions/cm^{2}sec ster MeV. The maximum counting rate was $\lesssim$ 25 times that measured by Helios-1 at the same time, i.e., comparable to the increase which Helios-2 observed at shock C, as described above. This increase may be due to: 1) particles accelerated by the shock, 2) flare particles trapped behind the shock, and/or 3) energetic storm particles. Following the shock, the counting rate again decreased until the interaction region of the corotating stream arrived at Helios-2, at

which time there was slight increase in the counting rate, perhaps due to compression in the interaction region. When the interface arrived, the counting rate at Helios-2 dropped rapidly (exponentially with a time scale of 3 hr) to approximately the same level that Helios-1 recorded. Apparently particles accelerated by shock A could not penetrate the stream interface and many were trapped in a region bounded by the interface on one side and the shock on another side. (The piston from the flare, assuming there was one, might have provided the third boundary.) The scenario that has been described is represented schematically in Figure 8.

Voyager-1, and -2 observed intensity-time profiles of protons in the energy range $\sim$ 50 keV - 138 keV (Figure 19) which resemble the profile recorded by Helios-2. During the early stage of the decay, both spacecraft observed a monotonic decrease in counting rate lasting $\sim$ 16 hrs. (The initial increase in counting rate and the first hour or two of the decay includes an uncertain contribution to energetic, omni-directional particles.) The counting rate then increased gradually during the next 8 days, reaching a maximum counting rate at the time that shock A arrived. (Recall that there was a data gap at Voyager-2 between 06:00 and 09:00 UT, so the shock was not observed directly.) This gradual increase lasted too long to be due to particles accelerated by the shock alone. Probably, energetic storm particles were present. The rapid increase several hours ahead of the shock at Voyager-1 and -2, however, is probably a contribution due to shock acceleration. The enhancement is relatively small, no more than about 16 times the ambient value. It did not extend above 0.5 MeV for protons. No modulation of electrons in the range 0.03 - 1.5 MeV was observed. At the time of the shock, Voyager-1 observed a strong anisotropy (3.5:1), the particles flowing away from the sun. Shortly after the shock passed, the anisotropy direction reversed and particles were observed to be streaming toward the sun, consistent with the hypothesis that most of the particles observed near the shock were accelerated by the shock. Following the shock, the counting rate decreased; rapidly at first and then more slowly. Shock B (see Section 2) arrived at Voyagers-1 and -2 during the decline in intensity, on November 29, and the corotating stream interface arrived several hours later. A very small increase in the counting rate of low energy protons was observed by Voyager-2 and an even smaller increase by Voyager-1, but those were insignificant compared to the other

shock-associated enhancements described above. A small increase in counting rate was observed in the interaction region ahead of the interface (Figure 19), analagous to that observed on November 25 by Helios-2 when it encountered the interaction region (Figure 18).

7. SUMMARY

We have presented a wealth of data obtained at $\gtrsim$ 0.6 AU, 1 AU, and 1.6 AU, describing the evolution and interactions of particles, flows, and fields in the period November 22, to December 6, 1977. Some of the principal results of our analysis of these data are the following:

1. A small, corotating stream, originating in a coronal hole, was observed to disappear as it moved from 0.7 AU to 1.6 AU. A forward shock, (shock B), was produced by the stream and observed by Helios-2 (0.6 AU), IMP-8 and Earth (1 AU) and Voyager-1, 2, which were nearly radially aligned; however, the shock was not corotating because it was not seen at Helios-1, 35° E of Helios 2. Apparently, the flow was corotating, but non-stationary. The stream interface corotated from 0.7 AU to 1.6 AU and persisted even though the stream had dissipated; it was stable and its structure remained essentially the same at all positions.

2. An exceptionally intense type III burst, produced by the November 22, 1977 flare, was observed by Helios-1 and -2. The electron beam which caused it, and plasma oscillations excited by the beam were observed at 0.6 AU.

3. The shock produced by the flare of November 22 (shock A) was non-spherical, pointing 34° to the E and 10° S of the radial direction at 1.6 AU. It interacted with another shock beyond 0.6 AU, and they coalesced forming a single shock that was observed at 1 AU and at 1.6 AU.

4. A shock of uncertain origin (shock C) was observed by 5 spacecraft at radial distances from the sun ranging from 0.6 to 1.6 AU and with longitudinal separations up to 36°. The radial distances versus time diagram suggested a spherical shock moving at a constant speed, but analysis of data at the shocks showed local fluctuations of up to 100 km/s in speed and 40° in direction.

5. One or more of three types of electrostatic waves were observed at interplanetary shocks: upstream waves with $f_p^- \lesssim f < f_p^+$, downstream waves with $f < f_p^-$, and broadband noise at the shock. These three types of

emissions were observed at 1.6 AU as well as 0.6 AU. The specific pattern varied greatly among the shocks observed, even for the same shock observed at closely separated ($\lesssim$ 0.2 AU) spacecraft, indicating a strong dependence on local shock and solar wind parameters.

6. Energetic protons ($\gtrsim$ 50 to 200 keV) were observed to be accelerated at shocks. The maximum and half widths of the flux profiles at a shock differed by approximately a factor of 2 over distances of a few tenths of an AU, indicating a dependence on local conditions. The data suggest a tendency for the fluxes to become broader and more intense with increasing distance from the sun.

7. Energetic protons ($\gtrsim$ 50 keV) from the November 22, 1977 flare were observed. Helios-1 observed that their intensity decayed monotonically in the corotating stream, with little change across the stream interface. Helios-2, 30° to the west of the interface, observed a very different profile, with a second increase to a maximum at the time the shock produced by the flare arrived. These "extra" particles apparently did not penetrate the interface, for the intensity at Helios-2 dropped abruptly to the intensity observed at Helios-1 when the interface corotated past Helios-2.

ACKNOWLEDGMENTS

This paper was made possible by the efforts of many people. The Project Leaders--Dr. H. Porsche, J. Trainor, A. Kutzer (DFVLR/ERNO) and Kochendorfer (NASA/HQ), representing Helios; Drs. E. Stone and M. Mitz (NASA/HQ), representing Voyager--made special efforts to coordinate the acquisition of Helios and Voyager data and to provide nearly complete data sets for the unique interval that we studied. The Workshop was proposed and organized by Dr. T. Krimigis. Four Principal Investigators, not listed as authors, generously provided us their data, which were essential for this study--Drs. H. Bridge, T. Krimigis, N. Ness, and R. Stone. The shocks were identified by the Workshop participants in presentations and round-table discussions. M. Denskat and Mr. Volkmer provided the data on the shock seen at Helios-2 on November 25.

REFERENCES

Abraham-Shrauner, B., and S. H. Yun, Interplanetary shocks seen by Ames plasma probe on Pioneer 6 and 7, J. Geophys. Res., 81, 2097, 1976.

Acuna, M. H., L. F. Burlaga, R. P. Lepping, and N. F. Ness, Initial results from the Voyagers 1, 2 magnetic field experiments, Contributions to the Fourth Solar Wind Conference, NASA/TM 79711; to appear in Proceedings of the Fourth Solar Wind Conference, 1979.

Alvarez, H., F. Haddock, and R. P. Lin, Evidence for electron excitation of type III radio burst emission, Solar Phys., 26, 468, 1972.

Belcher, J., and L. Davis, Jr., Large-amplitude Alfven waves in the interplanetary medium, 2, J. Geophys. Res., 76, 3534, 1971.

Burlaga, L. F., Interplanetary stream interfaces, J. Geophys. Res., 79, 3717, 1974.

Burlaga, L. F., Interplanetary streams and their interaction with the earth, Space Sci. Rev., 17, 327, 1975.

Burlaga, L. F., Magnetic fields, plasmas, and coronal holes: the inner solar system, NASA/TM 79598, 1978, to appear in Space Sci. Rev., 1979.

Burlaga, L. F., N. Ness, F. Mariani, B. Bavassano, U. Villante, H. Rosenbauer, R. Schwenn, and J. Harvey, Magnetic fields and flows between 1 AU and 0.3 AU during the primary mission of Helios 1, J. Geophys. Res., 83, 5167, 1978.

Burlaga, L. F., and J. D. Scudder, Motion of shocks through interplanetary streams, J. Geophys. Res., 80, 4004, 1975.

Chambon, G. Hurley, K., M. Niel, R. Talon, G. Vendrenne, O. B. Likine, A. V. Kovznetsov, and I. V. Estovline, A hard X-ray and gamma ray observation of the 22 November, 1977 solar flare, Colloques internatinaux du C.N.R.S. N^{O} 282-Contexte coronal des eruptions solaires.

Dryer, M., Interplanetary shock waves generated by solar flares, Space Sci. Rev., 15, 403, 1974.

Dryer, M., Z. K. Smith, E. J. Smith, J. D. Mihalov, J. H. Wolfe, R. S. Steinolfson, and S. T. Wu, Dynamic MHD modeling of solar wind corotating stream interaction regions observed by Pioneer 10 and 11, J. Geophys. Res., 83, 4347, 1978.

Dryer, M., Z. K. Smith, R. S. Steinolfson, J. D. Mihalov, J. H. Wolfe, and J. K. Chao, Interplanetary disturbances caused by the August 1972 solar flares as observed by Pioneer 9, J. Geophys. Res., 81, 4651, 1976.

Gold, T., Plasma and magnetic fields in the solar system, J. Geophys. Res., 64, 1665, 1959.

Gosling, J. T., A. J. Hundhausen, and S. J. Bame, Solar wind evolution at large heliocentric distances: Experimental demonstration and the test of a model, J. Geophys. Res., 81, 2111, 1976.

Gosling, J. T., J. R. Asbridge, S. J. Bame, and W. C. Feldman, Solar wind stream interfaces, J. Geophys. Res., 83, 1401, 1978.

Gurnett, D. A., and R. R. Anderson, Plasma wave electric fields in the solar wind: Initial results from Helios 1, J. Geophys. Res., 82, 632, 1977.

Gurnett, D. A., and L. A. Frank, Ion acoustic waves in the solar wind, J. Geophys. Res., 83, 58, 1978.

Gurnett, D. A., M. M. Baumback, and H. Rosenbauer, Stereoscopic direction finding analysis of a type III solar radio burst; evidence for emission at $2f_p^-$, J. Geophys. Res., 83, 616, 1978.

Gurnett, D. A. E. Marsch, W. Pilipp, R. Schwenn, and H. Rosenbauer, Ion acoustic waves and related plasma observations in the solar wind, J. Geophys. Res., 84, 2029, 1979a.

Gurnett, D. A., F. M. Neubauer, and R. Schwenn, Plasma wave turbulence associated with an interplanetary shock, J. Geophys. Res., 84, 541, 1979b.

Heineman, M. A., and G. L. Siscoe, Two-dimensional simulation of flare-associated disturbances in the solar wind, J. Geophys. Res., 79, 1349, 1974.

Hundhausen, A. J., Non-linear model of high-speed solar wind streams, J. Geophys. Res., 78, 1528, 1973.

Hundhausen, A. J., An interplanetary view of coronal holes, in Coronal Holes and High Speed Solar Wind Streams, edited by J. B. Zirker, p. 298, Colorado Associated Universities Press, Boulder, 1977.

Hundhausen, A. J., and L. F. Burlaga, A model for the origin of solar wind stream interfaces, J. Geophys. Res., 80, 1845, 1975.

Kurt, V. G., Yu I. Logacher, V. G. Stolpovskii, N. F. Pissarenko, M. Gros, A. Ranart, L. Trieger, and T. Gombosi, Analysis of energetic particle events following solar flares of September 24 and November 22, 1977, Tech. Report KFKI-1978-37, 1978.

Lepping, R. P., and P. D. Argentiero, Single spacecraft method of estimating shock normals, J. Geophys. Res., 76, 4349, 1971.

Lin, R. P., L. G. Evans, and J. Fainberg, Simultaneous observations of fast electrons and type III radio burst emissions near 1 AU, Astrophys. Letters, 14, 191, 1973.

Neubauer, F. M., Solar wind discontinuities, J. Geophys. Res., 13, 2248, 1976.

Ogilvie, K. W., Corotating shock structures, in Solar Wind, edited by C. P. Sonett, P. J. Coleman, Jr., and J. M. Wilcox, NASA SP-308, Washington, D. C., 1972.

Ogilvie, K. W., and L. F. Burlaga, A discussion of interplanetary post shock flows with two examples, J. Geophys. Res., 79, 2324, 1974.

Pizzo, V., An evaluation of corotating solar wind stream models, in Contributions to the Fourth Solar Wind Conference, NASA/TM 79711, p. 55, 1979, to appear in Proceedings of the Fourth Solar Wind Conference, 1979a.

Pizzo, V., A three-dimensional model of corotating streams in the solar wind II. hydrodynamic streams, submitted to J. Geophys. Res., 1979b.

Scarf, F. L., Wave-particle interaction phenomena associated with shocks in the solar wind, Proceedings of the De Feiter Memorial Symposium on the Study of Traveling Interplanetary Phenomena, D. Reidel, Hingham, Mass., 1978.

Scarf, F. L., R. W. Fredricks, L. A. Frank, C. T. Russell, P. J. Coleman, Jr., and M. Neugebauer, Direct correlations of large-amplitude waves with suprathermal protons in the upstream solar wind, J. Geophys. Res., 75, 7316, 1970.

Scarf, F. L., and D. A. Gurnett, A plasma wave investigation for the Voyager mission, Space Sci. Rev., 21, 289, 1977.

Scarf, F. L., D. A. Gurnett, W. S. Kurth, and R R. Shaw, Voyager 1, 2, plasma wave observations for the September 1977 storm period, UAG Report on the September 1977 and November 1977 Solar-Geophysical Activity, 1979.

Schwenn, R., M. D. Montgomery, H. Rosenbauer, H. Miggenrieder, K. H. Mulhauser, S. J. Bame, W. C. Feldman, and R. T. Hansen, Direct observations of the latitudinal extent of a high-speed stream in the solar wind, J. Geophys. Res., 83, 1011, 1978.

Siscoe, G. L. Structure and orientation of solar wind interaction fronts: Pioneer 6, J. Geophys. Res., 77, 27, 1972.

Smith, E. J., L. Davis, Jr., P. J. Coleman, Jr., D. S. Colburn, P. Dyal, and D. E. Jones, August 1972 solar-terrrestrial events: observations of interplanetary shocks at 2.2 AU, J. Geophys. Res., 7, 1077, 1977.

Smith, E. J. and J. H. Wolfe, Pioneer 10, 11 observations of evolving solar wind streams and shocks beyond 1 AU, in Study of Traveling Interplanetary Phenomenal 1977, M. A. Shea et al. (eds.), p. 227-257, D. Reidel Publishing Co., Dordrecht-Holland, 1977.

Steinolfson, R. S., M. Dryer, and Y. Nakagawa, Numerical MHD simulation of interplanetary shock pairs, J. Geophys. Res., 80, 1223, 1975.

TABLE 1

PRINCIPAL INVESTIGATORS

	Plasma Analyzer	Magnetometer	Magnetometer	Radio Waves	Plasma Waves	Plasma and Radio Waves	Energetic Particles
Helios-1	Rosenbauer	Neubauer	Mariani/Ness	Stone	Gurnett	Kellogg	Keppler
Helios-2	Rosenbauer	Neubauer	Mariani/Ness	Stone	Gurnett	Kellogg	Keppler
Voyager-1	Bridge	Ness			Gurnett		Krimigis
Voyager-2	Bridge	Ness			Gurnett		Krimigis
IMP-7	Bridge	Ness			Gurnett		
IMP-8	Bridge	Ness			Gurnett		

TABLE 2

STREAM INTERFACE

COROTATION

From	To	$\phi_2 - \phi_1$	$(r_2 - r_1)$ (AU)	$(t_2 - t_1)_{Predicted}$ (hr)	$(t_2 - t_1)_{Observed}$ (hr)
Helios-1 (11/23, 0245)	Helios-2 (11/25, 0721)	35.2°	-0.029	57	53
Helios-2	IMP (11/27, 02:00) ±01:00	$8.2^\circ \pm 0.1^\circ$	0.353	51	43 ± 1
IMP	Voy. 1 (11/29, 16:00) ±00:15	$-1.7^\circ \pm 0.8^\circ$	0.605	60 ± 3	62 ± 1
Voyager 1	Voy. 2 (11/29, 21:25)	0.9°	0.012	3	5

TABLE 3

SHOCK B

	Helios 2	SSC	Voy. 1	Voy. 2
Shock ID	B_1	B_2	B_3	B_4
Date	Nov. 25	Nov. 26	Nov. 29	Nov. 29
Hr: min.	01:47	17:04	02:04	07:21
$r(10^8 km)$	0.944	1.476	2.373	2.390
Normal λ_n	60^o	--	9.1^o	14.9^o
Normal δ_n	14^o	--	-0.7^o	21.2^o
V(km/s)	300	--	409	395
V_r(km/s)	540	--	409	423

TABLE 4

SHOCK A

	Helios 2	Helios 2	Helios 1	IMP-8	Voy. 2	Voy. 1
Shock I.D.	A_1	A_2	A_3	A_4	A_5	A_6
Date	Nov. 23	Nov. 24	Nov. 25	Nov. 25	Nov. 27	Nov. 27
Hr: min	16:10	06:11	22:28	12:13	07:30 $\pm$ 01:30	22:26
$r(10^8$ km)	0.916	0.927	1.018	1.476	2.361	2.533
Normal λ_n	16^o	-15^o	4^o			-34^o
Normal θ_n or δ_n	$\theta_n = -14$	$\theta_n = -48^o$	$\theta_n = 25^o$			$\delta_n = -10^o$
V(km/s)	330	304	352			302
V_r(km/s)	353	467	390	$\sim$ 418		369

TABLE 5

SHOCK C

SHOCK I.D.	Helios 2 C_1	Helios 1 C_2	IMP 7 C_3	Voy. 2 C_4	Voy. 1 C_5
Date	Dec. 1	Dec. 1	Dec. 2	Dec. 3	Dec. 3
Hr: min	01:29	05:14	02:15	21:41	23:18
r(10^8 km)	1.042	1.111	---	2.455	2.445
Normal λ_n	-3°	3°	---	38.3°	---
Normal θ_n	17°	-34°	---	-6°	---
V(km/s)	441	417	---	415	---
V_r(km/s)	460	501	---	530	---

FIGURE CAPTIONS

FIGURE 1 Ecliptic plane projection of the trajectories of Helios-1, -2 and Voyager-1, -2 shown in the inertial solar ecliptic coordinate system for the interval November 22 - December 6, 1977.

FIGURE 2 Corotating interface. The top panel shows the associated stream relative to the interface at each spacecraft. The bottom panel shows the intersection of the interface with the ecliptic plane at the time that it passed each of the spacecraft. The dashed circular arc passing through Earth represents Earth's orbit. The position of shock B is also shown, and its orientation is illustrated in the bottom panel.

FIGURE 3 The corotating stream interface (top) seen by each of the spacecraft. The interface is defined by the abrupt decrease in density and the corresponding increase in temperature. Times have been shifted so that the interfaces are aligned vertically, allowing a comparison of the density, temperature, and magnetic field intensity profiles (bottom).

FIGURE 4 Structure of the interface, shown by a plot of high resolution magnetic field and plasma data (top), and corresponding plasma wave observations. The interface is relatively broad (30 min), its structure does not change appreciably over the 0.2 AU separation between Voyager-1 and Voyager-2, and there is no evidence of an instability that might produce waves $\lesssim f_p^+$ at Voyager-2.

FIGURE 5 Shock B, showing the high-resolution magnetic field and plasma data (top panel) and plasma wave observations (bottom panel) near the shock. The flow and field parameters are steady before and after the shock front, allowing accurate determination of its normal and speed. Whistler wave

turbulence is observed at $f < f_p^+$ behind the shock; a short burst of broadhand turbulence is observed at the shock; and "ion-acoustic" waves are observed at $f_p^+ < f < f_p^-$ ahead of the shock.

FIGURE 6 A type III burst (77 kHz to 3000 kHz), the beam of electrons (20-65 keV) which produced the burst, and plasma waves (at the local plasma frequency, 52 kHz) produced locally by the electron beam. The profiles at 52, 77 and 203 kHz are from the University of Minnesota experiment; the others are from the Goddard Space Flight Center experiment on Helios-2.

FIGURE 7 Shocks A_1, A_2, A_3 and the stream interface. At 0600 UT, November 24, 1977, the interface had passed Helios-1, but had not reached Helios-2. One shock (A_3) was approaching Helios-1 and arrived at Helios-1 late on November 24. Two shocks were observed by Helios-2. One (A_2) arrived at Helios-2 at 0611 UT on November 24, and another was a short distance ahead of it. A_1 and A_2 coalesced into 1 shock (A_4) as they moved from Helios-1 to earth, where A_4 was detected by IMP-8.

FIGURE 8 A sketch, approximately to scale, showing the position of shock B, the stream interface, and shock A_2 at 0600 UT, when A_2 was approaching Helios-2. The positions of the spacecraft and the flare site at that time are also shown. The hypothetical piston was not observed. The flare produced energetic protons which escaped freely through the stream. Shock A_2 accelerated particles locally and perhaps trapped some of the flare particles, producing a local maximum in counting rates at the shock observed by Helios-2. These shock-accelerated particles did not penetrate the stream interface and were not observed by Helios-1.

FIGURE 9 Propagation of shock A. The radial position of the shock is shown at the times that the shocks arrived at Helios-1 (H1), Helios-2 (H2), IMP-8, Voyager-1 (V1) and Voyager-2 (V2). The two shocks observed by H2 coalesced into the one shock observed by IMP-8. Departures from spherical symmetry of shock A are indicated by the scatter of the points about a straight line.

FIGURE 10 High resolution magnetic field and plasma data show that A_4 (at IMP-8) and A_6 (at Voyager-1) are shocks. A narrow, broadband burst of electrostatic noise was observed at the time of the shock by both spacecraft. "Ion-acoustic" waves between f_p^- and f_p^+ were observed upstream by both spacecraft. Voyager-1 also observed whistler mode turbulence at $f < f_p^+$ behind the shock.

FIGURE 11 High resolution magnetic field and plasma data showing that A_1 and A_2 are shocks (or steep compressive waves). Electrostatic plasma wave data from Helios-2 show that the shock was imbedded in a broad region of doppler-shifted "ion-acoustic" waves. A narrow spike was observed at 562 and 311 Hz at the time of the shock.

FIGURE 12 High resolution plasma and magnetic field data showing shock C and a boundary behind it, which might be the piston boundary. Note the depressionn in magnetic field intensity at the boundary. Electrostatic plasma waves are observed between f_p^- and f_p^+ at the shock, but no significant waves are observed at the "piston boundary".

FIGURE 13 Sixteen-min. averages of the speed, density, temperature, and magnetic field intensity, showing shock C, the pre- and post-shock conditions, and the post-shock conditions at Helios-1, -2 and at Voyager-1, -2. Note the drop in density and temperature and the high magnetic field intensities behind the shock at Helios-1 and -2, suggesting entry into a piston.

The parameters slowly decrease behind the shock at Voyager-1, -2, to the pre-shock levels, indicating that those spacecraft did not penetrate the piston.

FIGURE 14 High resolution magnetic field data showing shock C. The plasma wave data show a short broadband burst at Helios-2, but not at Voyager-2. Electrostatic waves were observed behind shock C at frequencies between 311 Hz - 17.8 kHz by Helios-2, and over a more limited frequency range (178 Hz - 5.62 kHz) by Voyager-2.

FIGURE 15 A sketch, drawn approximately to scale, illustrating the position of shock B, corresponding stream interface, the position of shock C and the corresponding piston at hour 0 on November 30, 1977. The positions of Helios-1, -2, Voyager-1, -2, and Earth at this time are also shown.

FIGURE 16 Propagation of shock C. The radial distance at the times that the shock passed each of the spacecraft are shown. The straight line fit suggests a uniform speed of 555 km/s and spherical symmetry, but local observations indicate appreciable scatter about those values.

FIGURE 17 Counting rates of energetic protons near shock C, observed by Helios-1, -2 and Voyager-1, -2. The broad, intense fluxes of particles at Voyagers-1 and -2 closely resemble one another, but they differ appreciably from the narrower, less intense fluxes observed by Helios-1 and -2. The Helios-2 profile differs appreciably from that of Helios-1. The abrupt decrease in counting rates behind the shock observed by Helios-1 and Helios-2 may be due to a flow boundary (e.g., a piston) behind the shock.

FIGURE 18 Counting rates of energetic protons produced by the November 22 flare and by shock A, as observed by Helios-1 and -2. The speed profiles are shown as an aid in describing the corresponding flows. Helios-1 and Helios-2 observed similar intensity-time profiles during the initial stage of the decay. Helios-1, which was in the corotating stream continued to observe an uninterrupted, monotonic decay to the background level three days later. Helios-2 observed a second increase of flux. The intensity dropped abruptly when the interface arrived, because the accelerated particles did not penetrate the interface.

FIGURE 19 Counting rates of energetic protons observed by Voyager-1 and -2. Speed profiles are shown to indicate the flow conditions. Both Voyager-1 and -2 observed flare particles on November 22. The broad increase between November 27 - November 29 may be due to energetic storm particles. Locally accelerated particles are observed at the trasient shock A, but there is no significant increase at the stationary shock B.

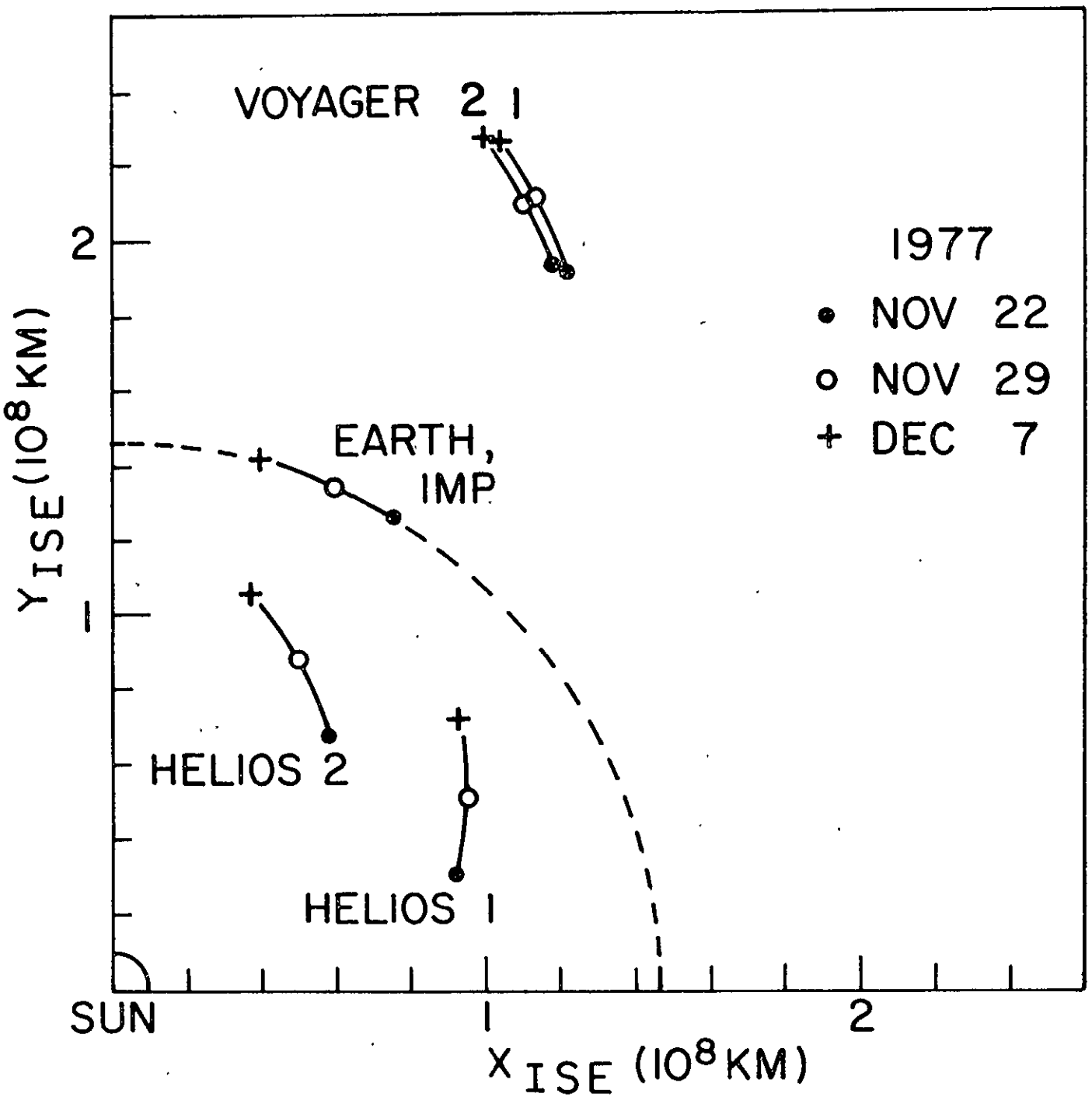
VOYAGER 2
1
1977
NOV 22
NOV 29
DEC 7
EARTH,
IMP
HELIOS 2
HELIOS 1
SUN
1
2
2
1
$Y_{ISE}(10^8 KM)$
$X_{ISE}(10^8 KM)$

Figure 1

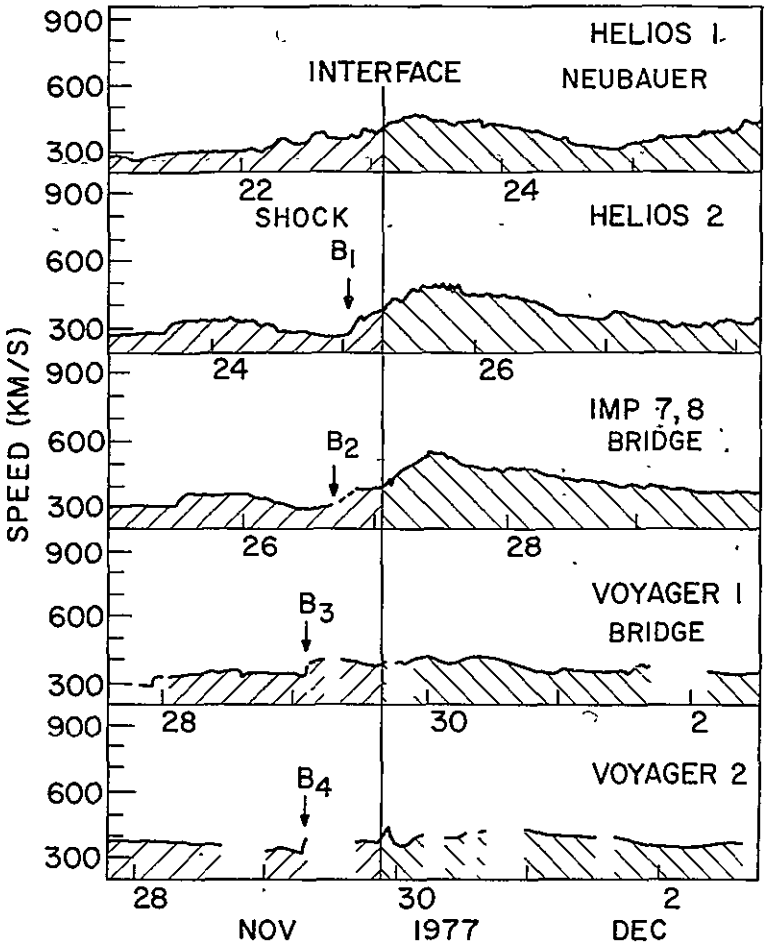
SPEED (KM/S)
900
600
300
HELIOS 1
INTERFACE
NEUBAUER
22
24
SHOCK
HELIOS 2
B1
24
26
IMP 7,8
BRIDGE
B2
26
28
VOYAGER 1
BRIDGE
B3
28
30
2
VOYAGER 2
B4
28
30
2
NOV
1977
DEC

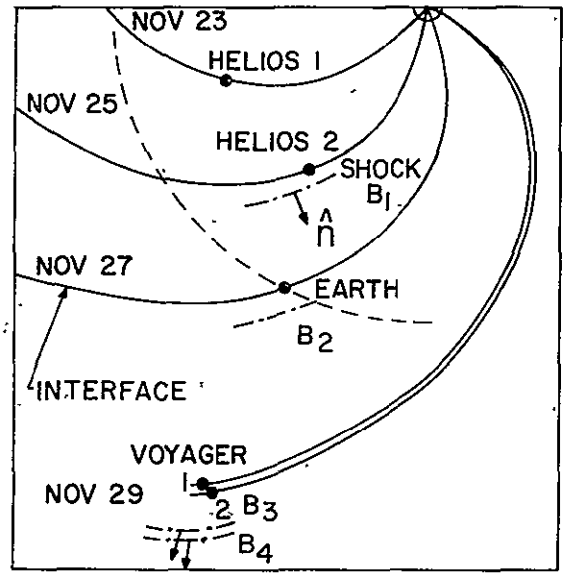
NOV 23
HELIOS 1
NOV 25
HELIOS 2
SHOCK
B1
n̂
NOV 27
EARTH
B2
INTERFACE
VOYAGER
1
NOV 29
2
B3
B4

Figure 2

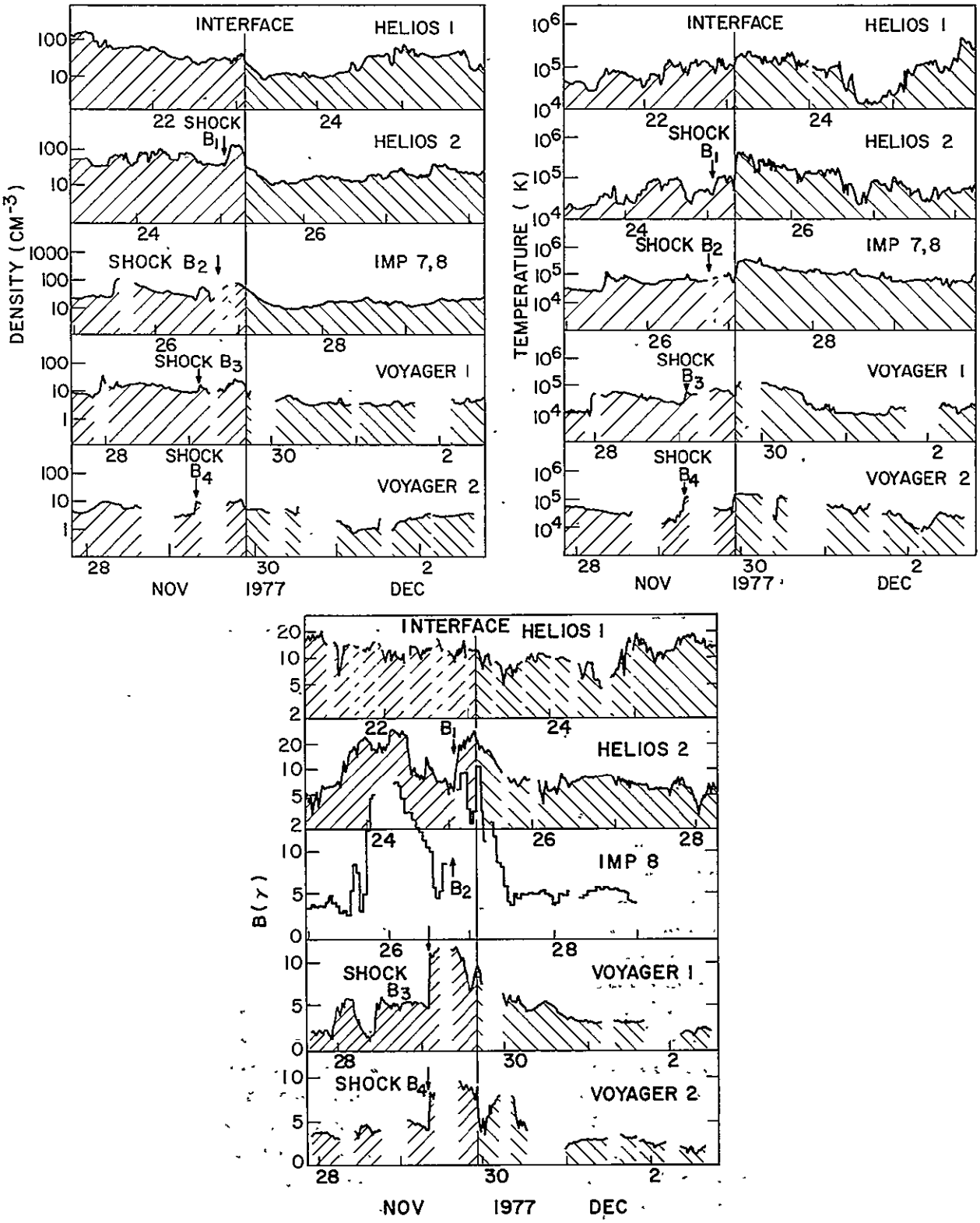
INTERFACE
HELIOS 1
22 SHOCK B1
HELIOS 2
SHOCK B2
IMP 7,8
SHOCK B3
VOYAGER 1
SHOCK B4
VOYAGER 2
DENSITY (CM-3)
TEMPERATURE (K)
B(γ)
NOV
1977
DEC

Figure 3

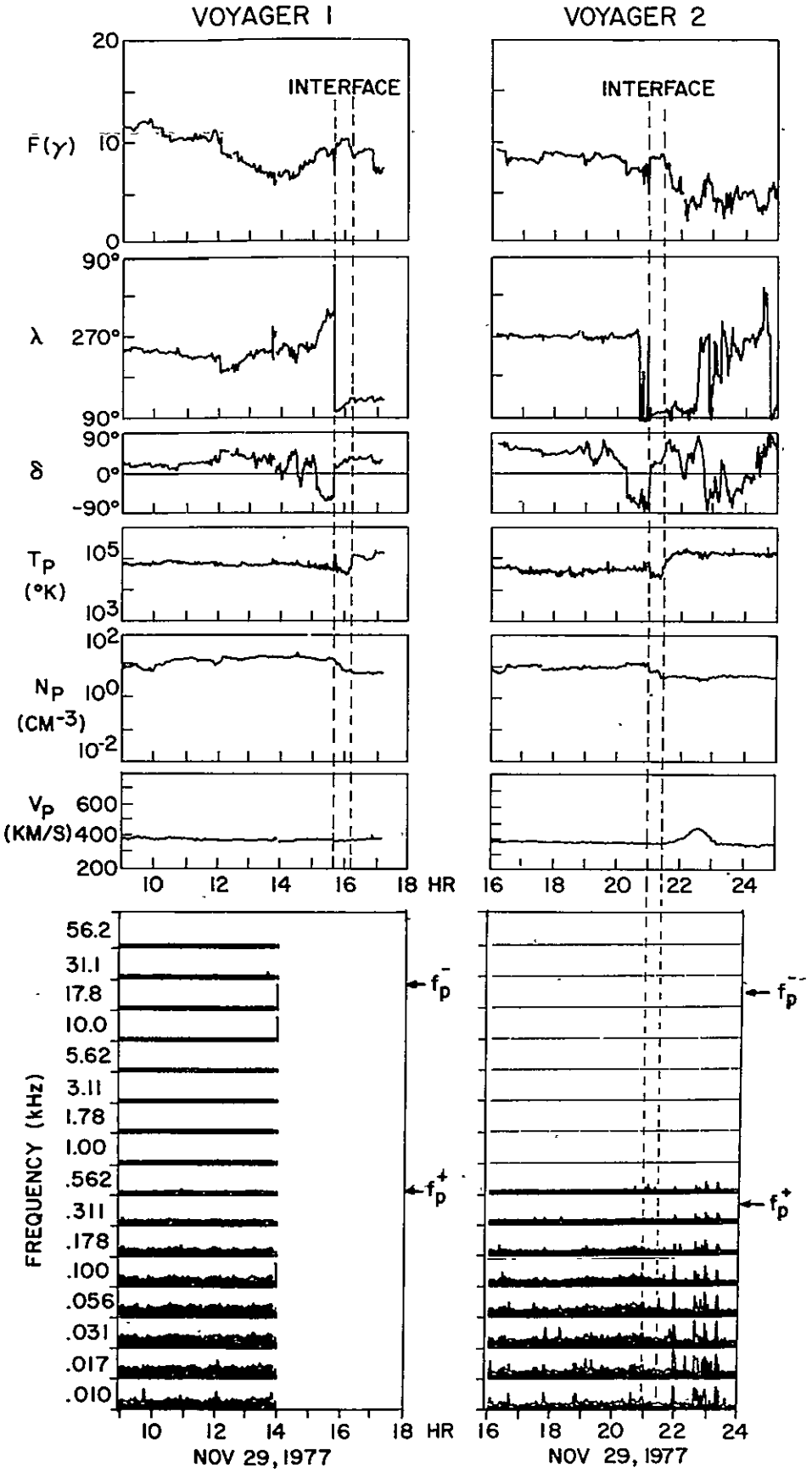
VOYAGER 1
VOYAGER 2
INTERFACE
INTERFACE
F(γ)
λ
δ
T_P (°K)
N_P (CM^{-3})
V_P (KM/S)
FREQUENCY (kHz)
f_p^-
f_p^+
HR
NOV 29, 1977
NOV 29, 1977

Figure 4

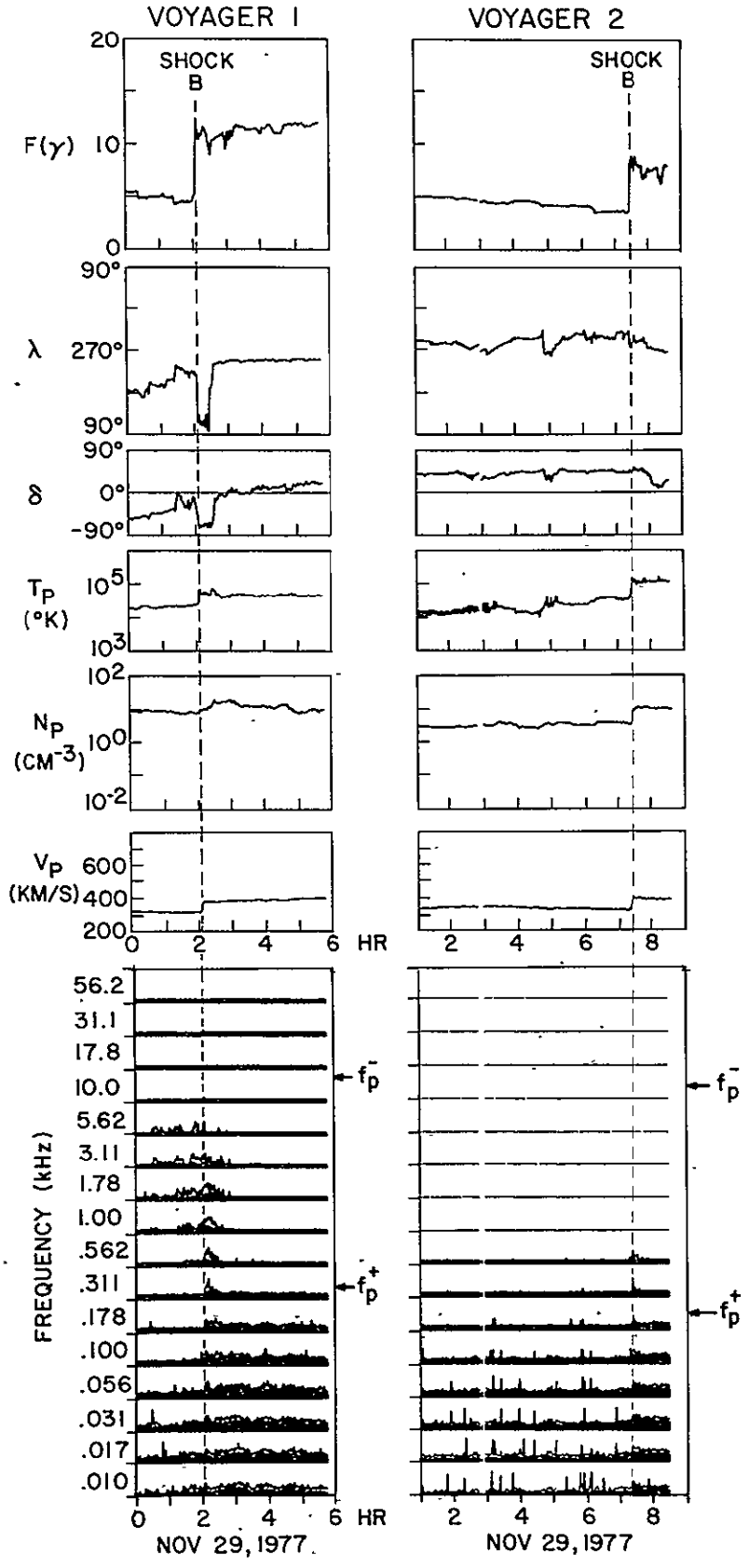
VOYAGER 1
VOYAGER 2
SHOCK
B
SHOCK
B
F(γ)
20
10
0
λ
90°
270°
90°
δ
90°
0°
-90°
T_P
(°K)
10^5
10^3
N_P
(CM^{-3})
10^2
100
10^{-2}
V_P
(KM/S)
600
400
200
0 2 4 6 HR
2 4 6 8
FREQUENCY (kHz)
56.2
31.1
17.8
10.0
5.62
3.11
1.78
1.00
.562
.311
.178
.100
.056
.031
.017
.010
f_p^-
f_p^+
0 2 4 6 HR
NOV 29, 1977
2 4 6 8
NOV 29, 1977

Figure 5

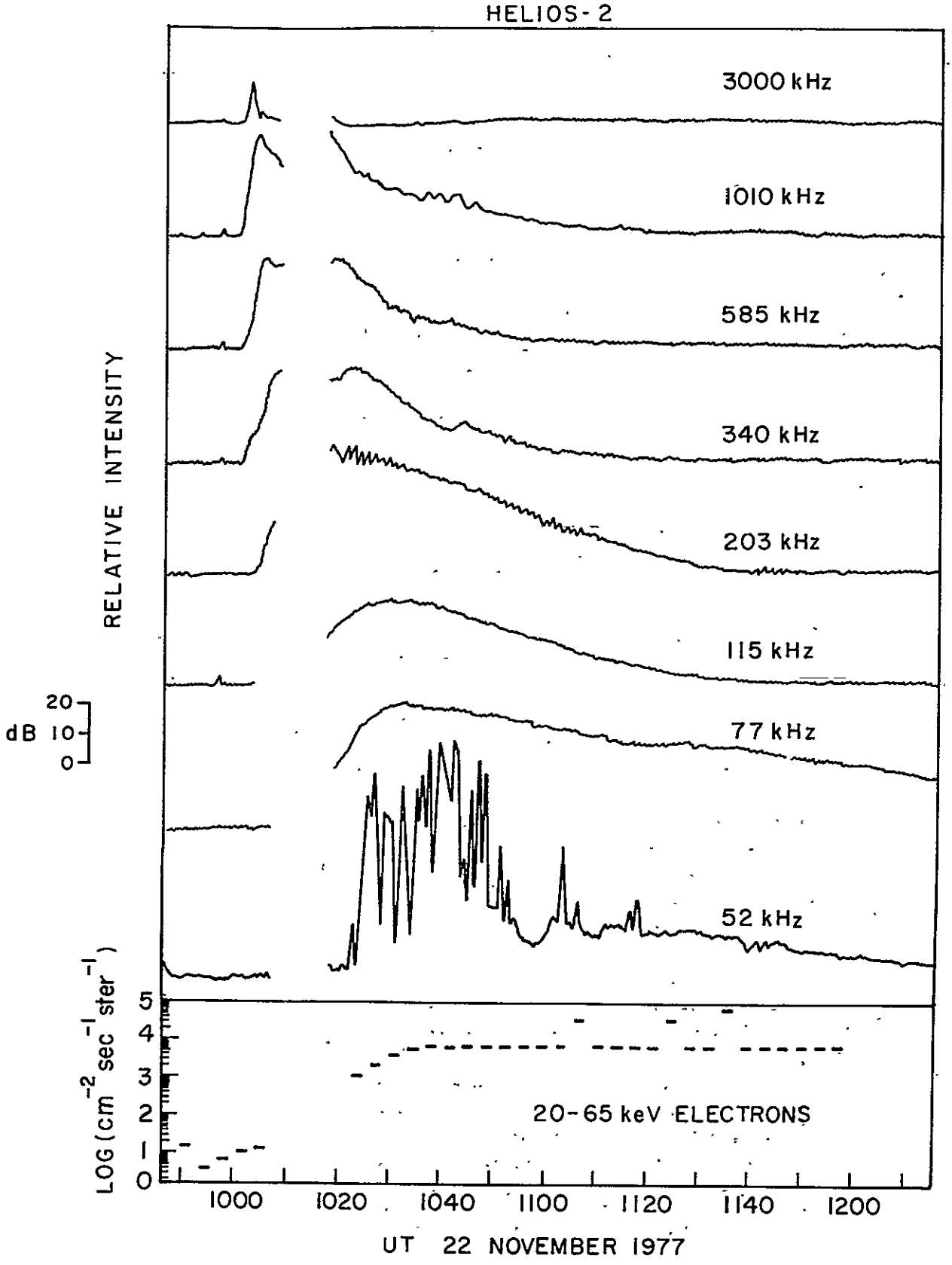
HELIOS-2
3000 kHz
1010 kHz
585 kHz
340 kHz
203 kHz
115 kHz
77 kHz
52 kHz
RELATIVE INTENSITY
20
dB 10
0
LOG (cm^{-2} sec^{-1} ster^{-1})
5
4
3
2
1
0
20-65 keV ELECTRONS
1000
1020
1040
1100
1120
1140
1200
UT 22 NOVEMBER 1977

Figure 6

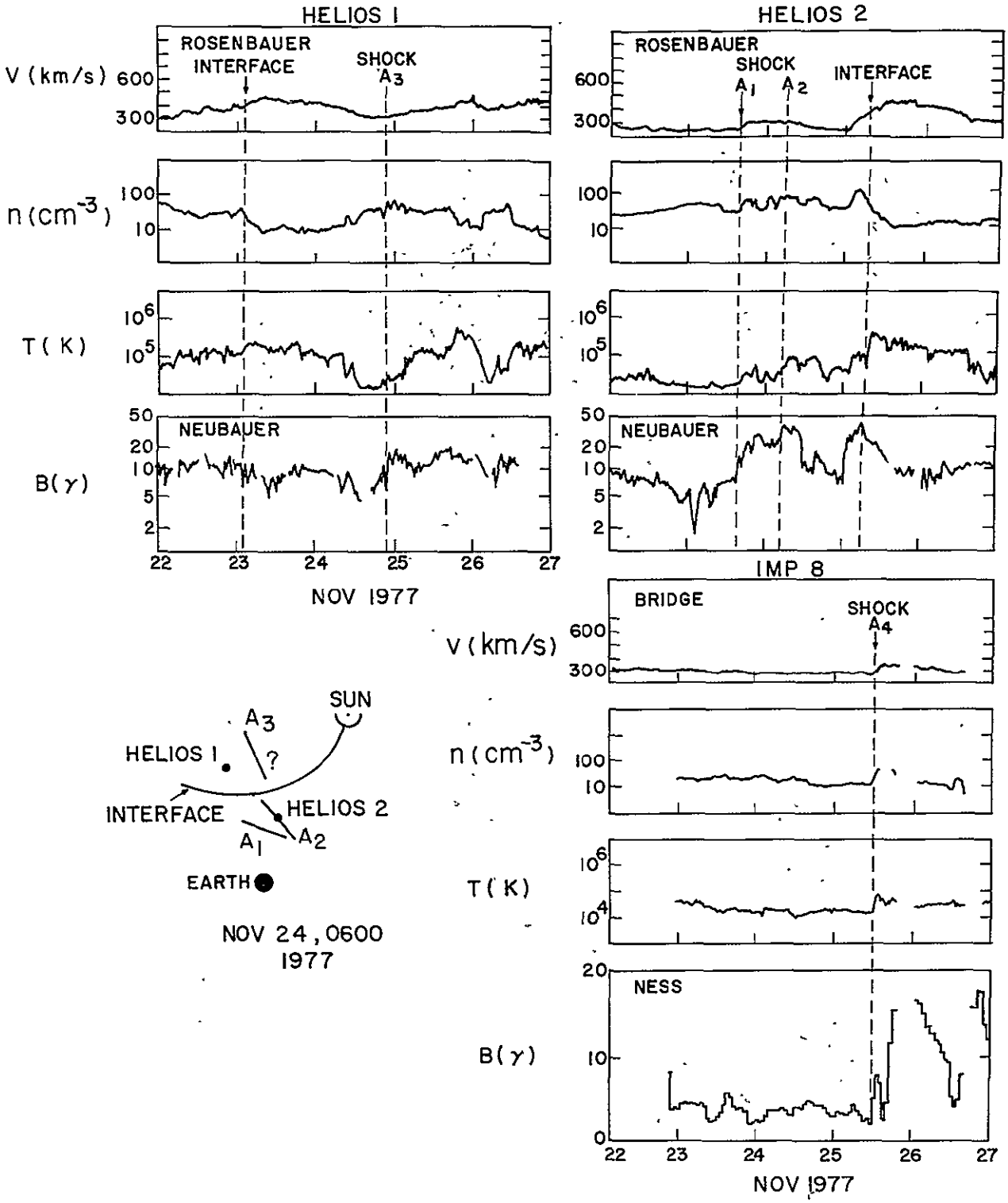
HELIOS 1
HELIOS 2
ROSENBAUER
INTERFACE
SHOCK
A3
A1
A2
V (km/s)
600
300
n(cm-3)
100
10
T(K)
10^6
10^5
NEUBAUER
B(γ)
50
20
10
5
2
22
23
24
25
26
27
NOV 1977
IMP 8
BRIDGE
v (km/s)
n (cm-3)
10^4
NESS
0
SUN
HELIOS 1
?
INTERFACE
HELIOS 2
EARTH
NOV 24, 0600
1977

Figure 7

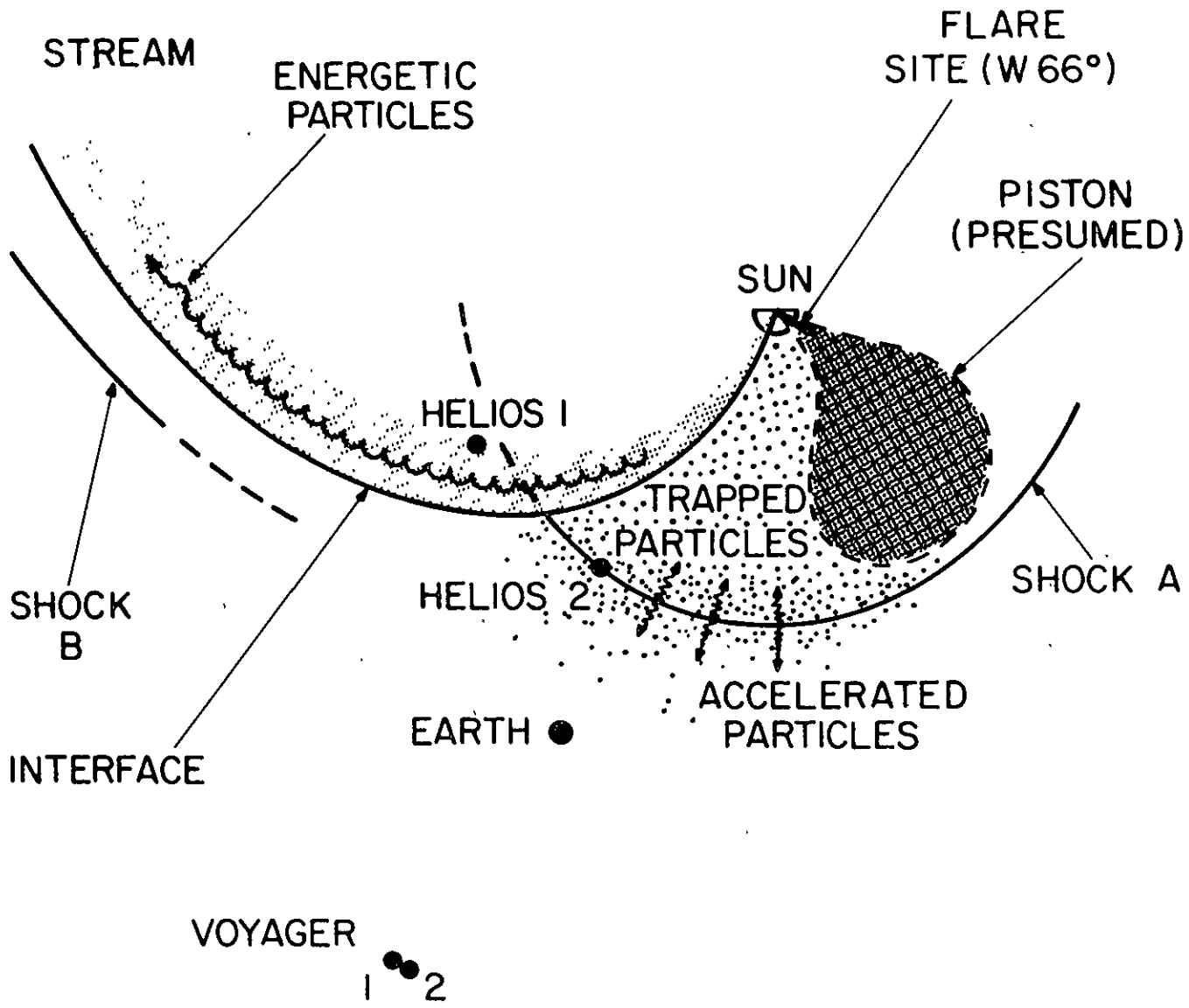
NOV 24, 1977
0600 UT
STREAM
ENERGETIC PARTICLES
FLARE SITE (W 66°)
PISTON (PRESUMED)
SUN
HELIOS 1
TRAPPED PARTICLES
HELIOS 2
SHOCK A
SHOCK B
INTERFACE
EARTH
ACCELERATED PARTICLES
VOYAGER
1
2

Figure 8

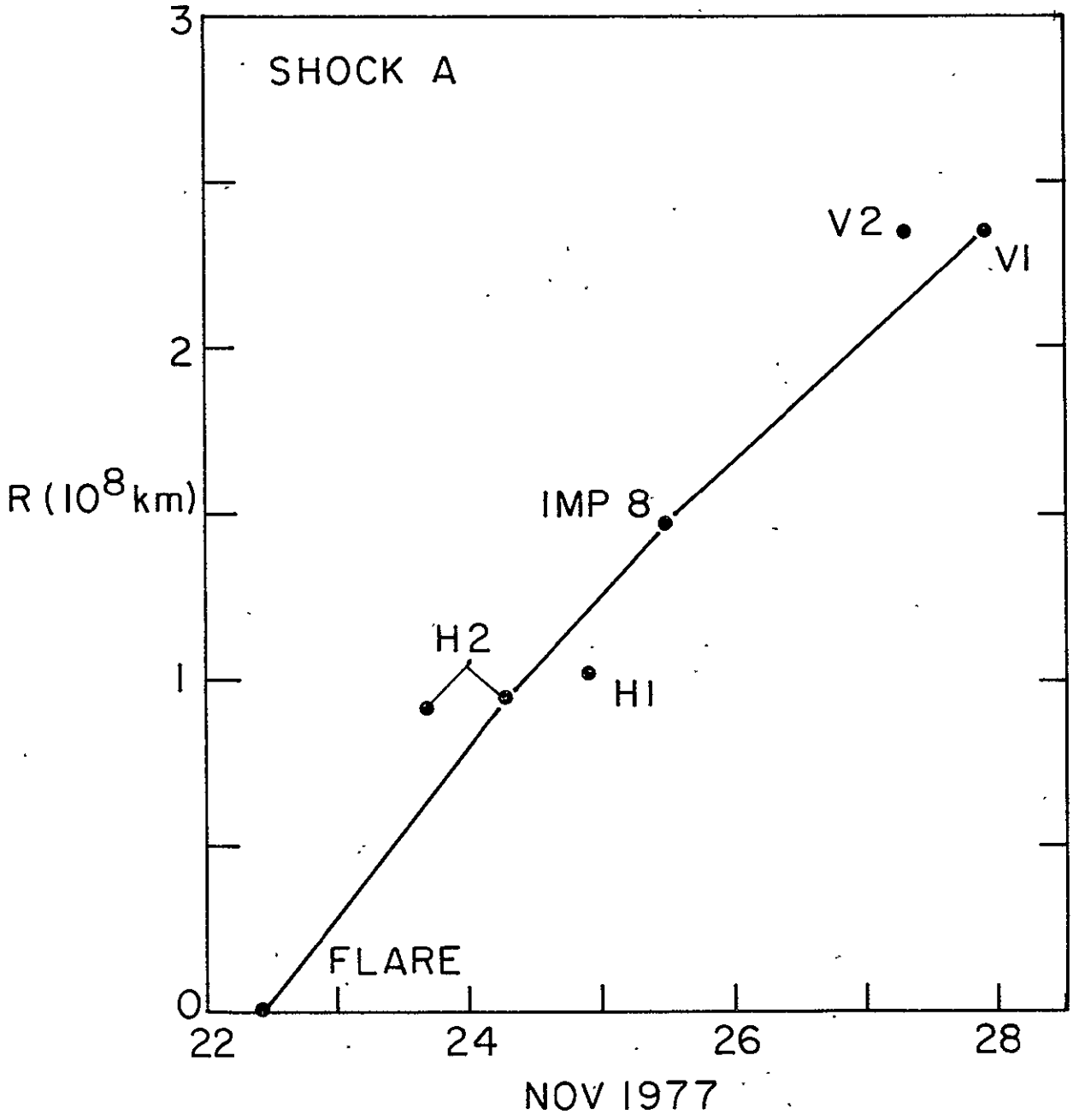

Figure 9

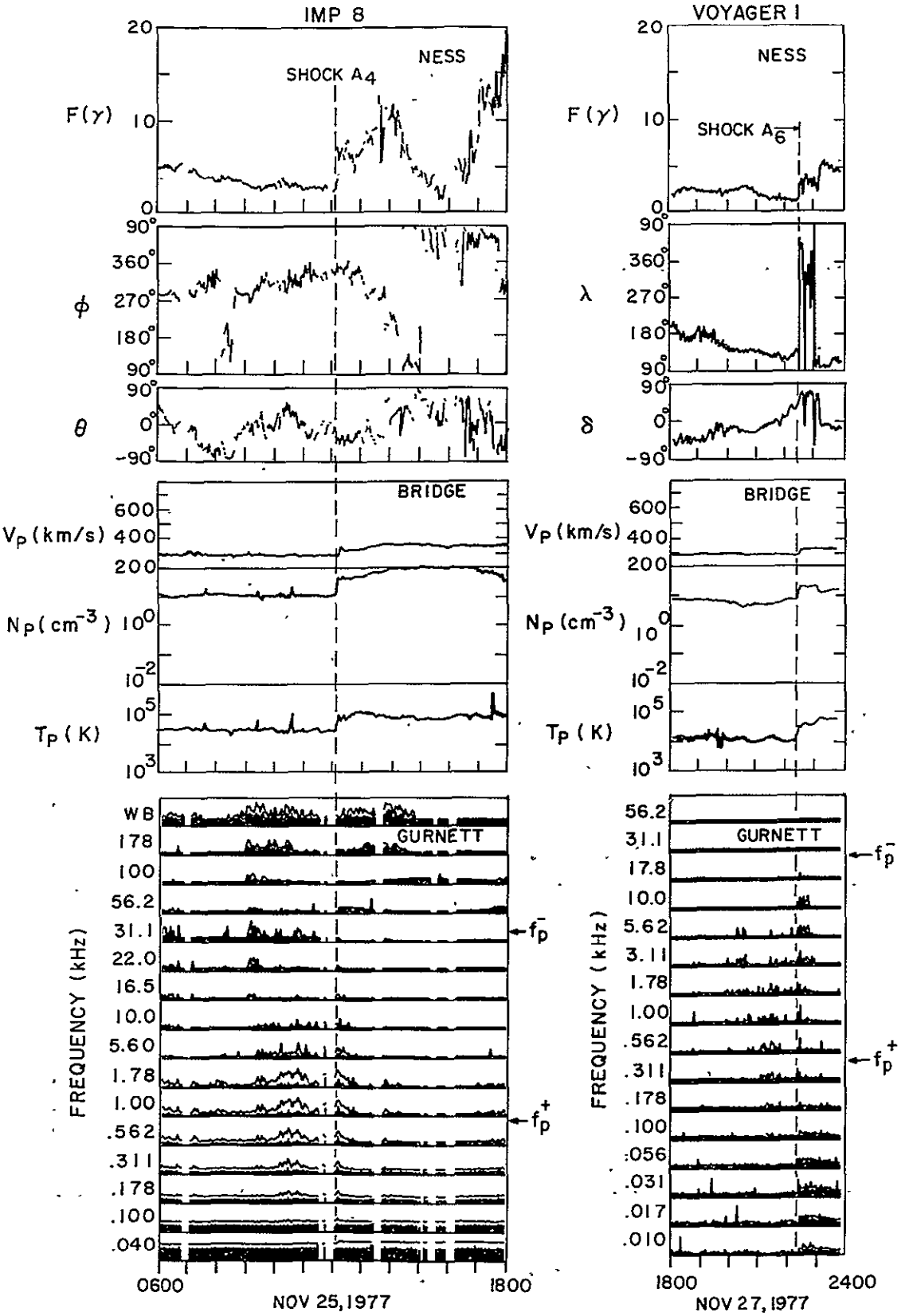
IMP 8
VOYAGER 1
NESS
SHOCK A4
SHOCK A6
F(γ)
φ
λ
θ
δ
BRIDGE
Vp (km/s)
Np (cm-3)
Tp (K)
GURNETT
WB
FREQUENCY (kHz)
fp-
fp+
0600
1800
NOV 25, 1977
1800
2400
NOV 27, 1977

Figure 10

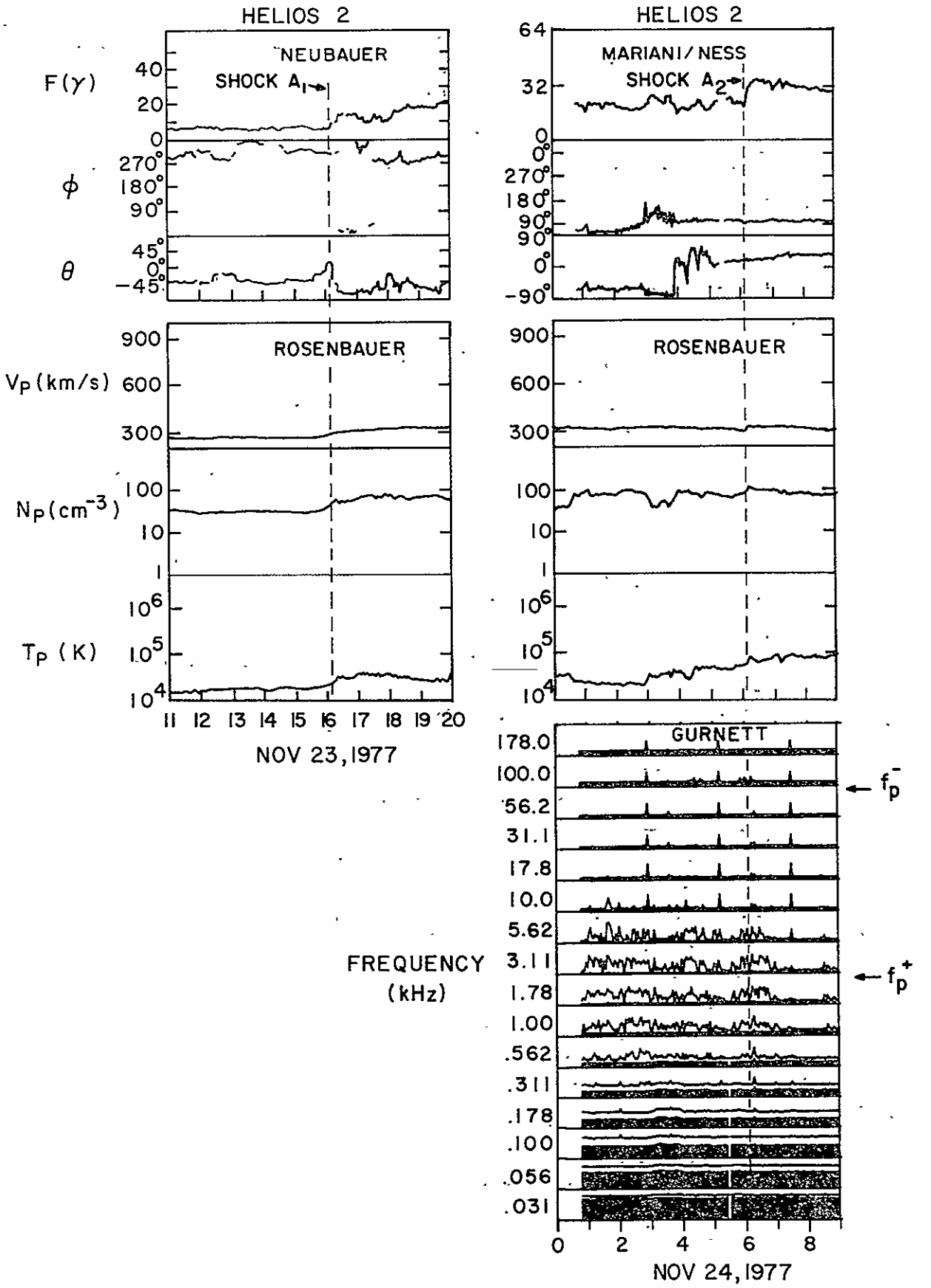
HELIOS 2
NEUBAUER
SHOCK A1
F(γ)
40
20
0
φ
270°
180°
90°
θ
45°
0°
-45°
HELIOS 2
MARIANI/NESS
SHOCK A2
64
32
0
0°
270°
180°
90°
90°
0°
-90°
ROSENBAUER
Vp (km/s)
900
600
300
Np (cm-3)
100
10
1
Tp (K)
10^6
10^5
10^4
ROSENBAUER
900
600
300
100
10
1
10^6
10^5
10^4
11 12 13 14 15 16 17 18 19 20
NOV 23, 1977
GURNETT
FREQUENCY
(kHz)
178.0
100.0
56.2
31.1
17.8
10.0
5.62
3.11
1.78
1.00
.562
.311
.178
.100
.056
.031
← fp-
← fp+
0 2 4 6 8
NOV 24, 1977

Figure 11

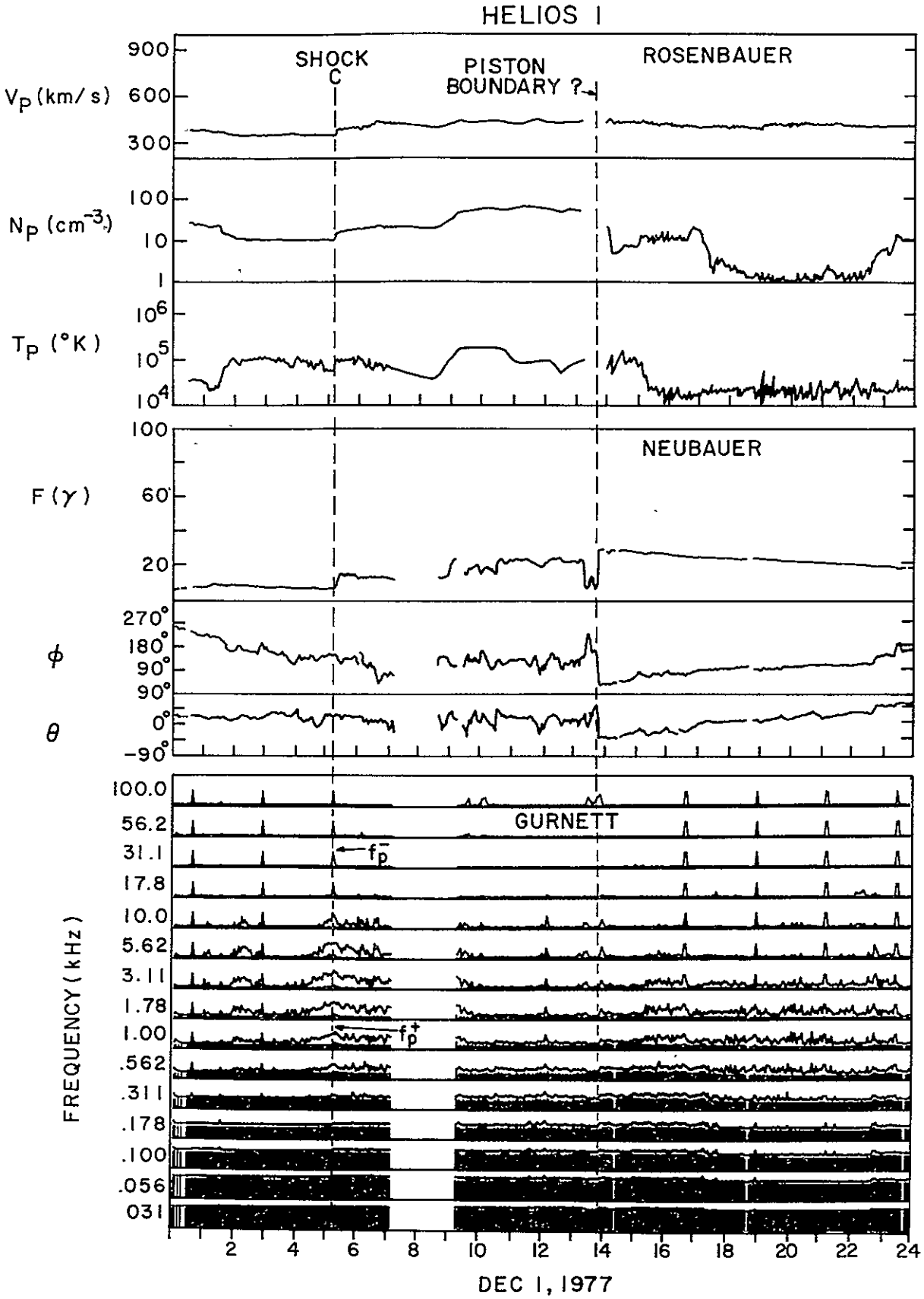
HELIOS I
SHOCK
C
PISTON
BOUNDARY ?
ROSENBAUER
NEUBAUER
GURNETT
V_P (km/s)
900
600
300
N_P (cm^{-3})
100
10
1
T_P (°K)
10^6
10^5
10^4
F(γ)
100
60
20
φ
270°
180°
90°
90°
θ
0°
-90°
FREQUENCY (kHz)
100.0
56.2
31.1
17.8
10.0
5.62
3.11
1.78
1.00
.562
.311
.178
.100
.056
031
f_p^-
f_p^+
2
4
6
8
10
12
14
16
18
20
22
24
DEC 1, 1977

Figure 12

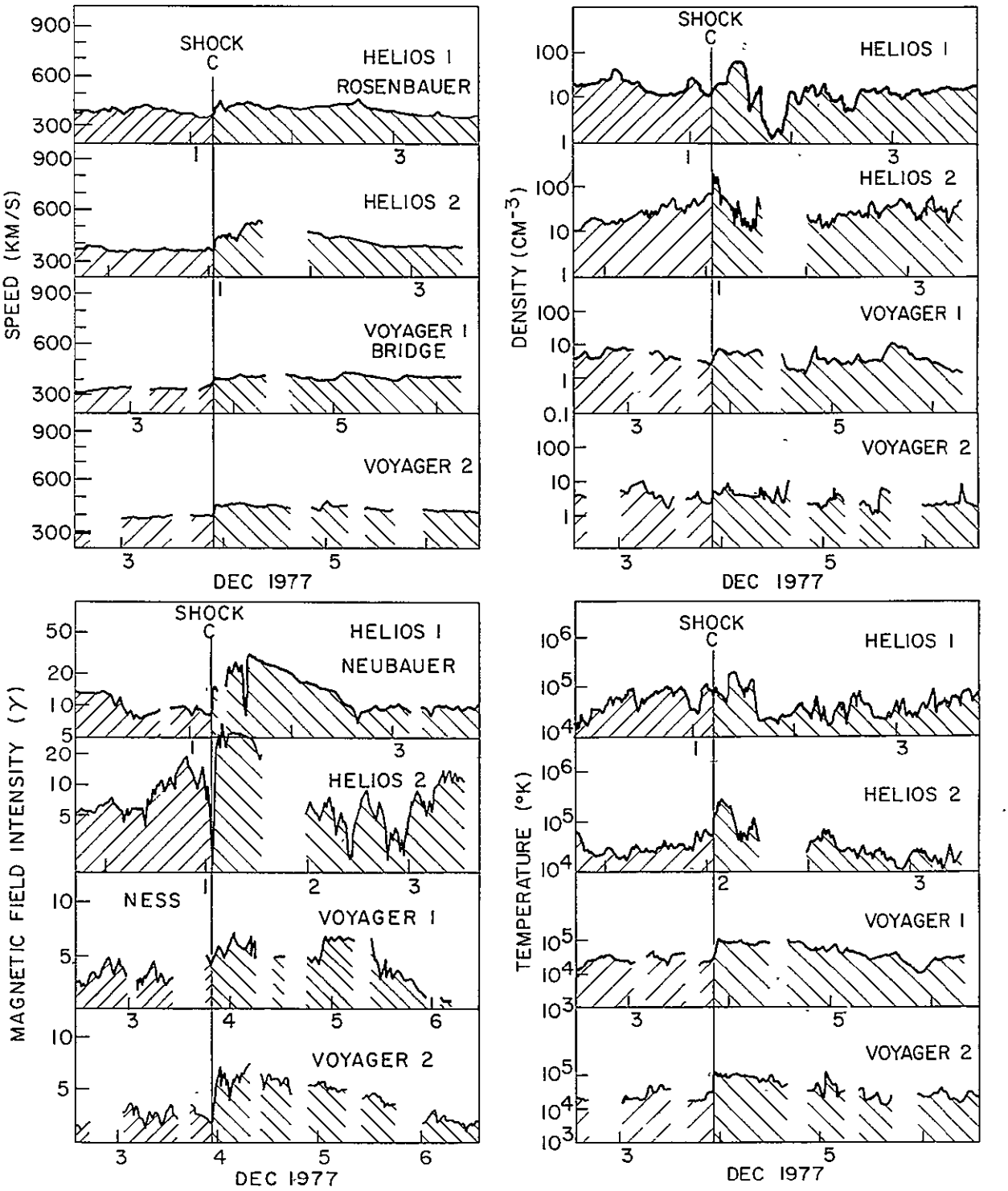
SPEED (KM/S)
SHOCK
C
HELIOS 1
ROSENBAUER
HELIOS 2
VOYAGER 1
BRIDGE
VOYAGER 2
DEC 1977
DENSITY (CM-3)
HELIOS 1
HELIOS 2
VOYAGER 1
VOYAGER 2
DEC 1977
MAGNETIC FIELD INTENSITY (γ)
HELIOS 1
NEUBAUER
HELIOS 2
NESS
VOYAGER 1
VOYAGER 2
DEC 1977
TEMPERATURE (°K)
HELIOS 1
HELIOS 2
VOYAGER 1
VOYAGER 2
DEC 1977

Figure 13

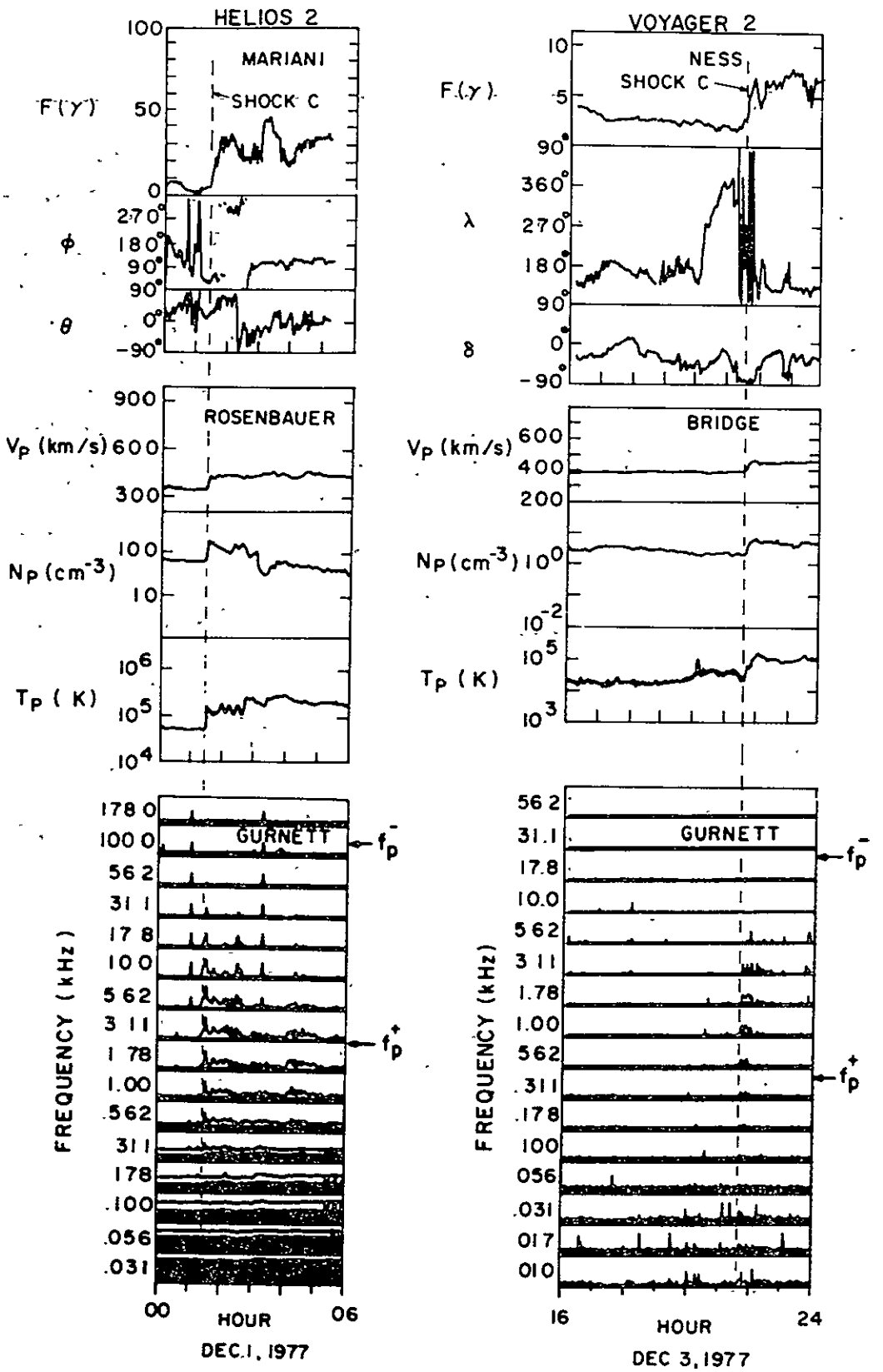
HELIOS 2
MARIANI
SHOCK C
F(γ)
100
50
0
φ
270°
180°
90°
θ
90°
0°
-90°
ROSENBAUER
Vp (km/s)
900
600
300
Np (cm-3)
100
10
Tp (K)
10^6
10^5
10^4
GURNETT
178 0
100 0
562
31 1
17 8
100
5 62
3 11
1 78
1.00
.562
311
178
.100
.056
.031
f_p^-
f_p^+
FREQUENCY (kHz)
00
HOUR
06
DEC.1, 1977
VOYAGER 2
NESS
SHOCK C
F(γ)
10
5
λ
90°
360°
270°
180°
90°
δ
0°
-90°
BRIDGE
Vp (km/s)
600
400
200
Np (cm-3)
10^0
10^-2
Tp (K)
10^5
10^3
GURNETT
56 2
31.1
17.8
10.0
5 62
3 11
1.78
1.00
562
.311
.178
100
056
.031
017
010
f_p^-
f_p^+
FREQUENCY (kHz)
16
HOUR
24
DEC 3, 1977

Figure 14

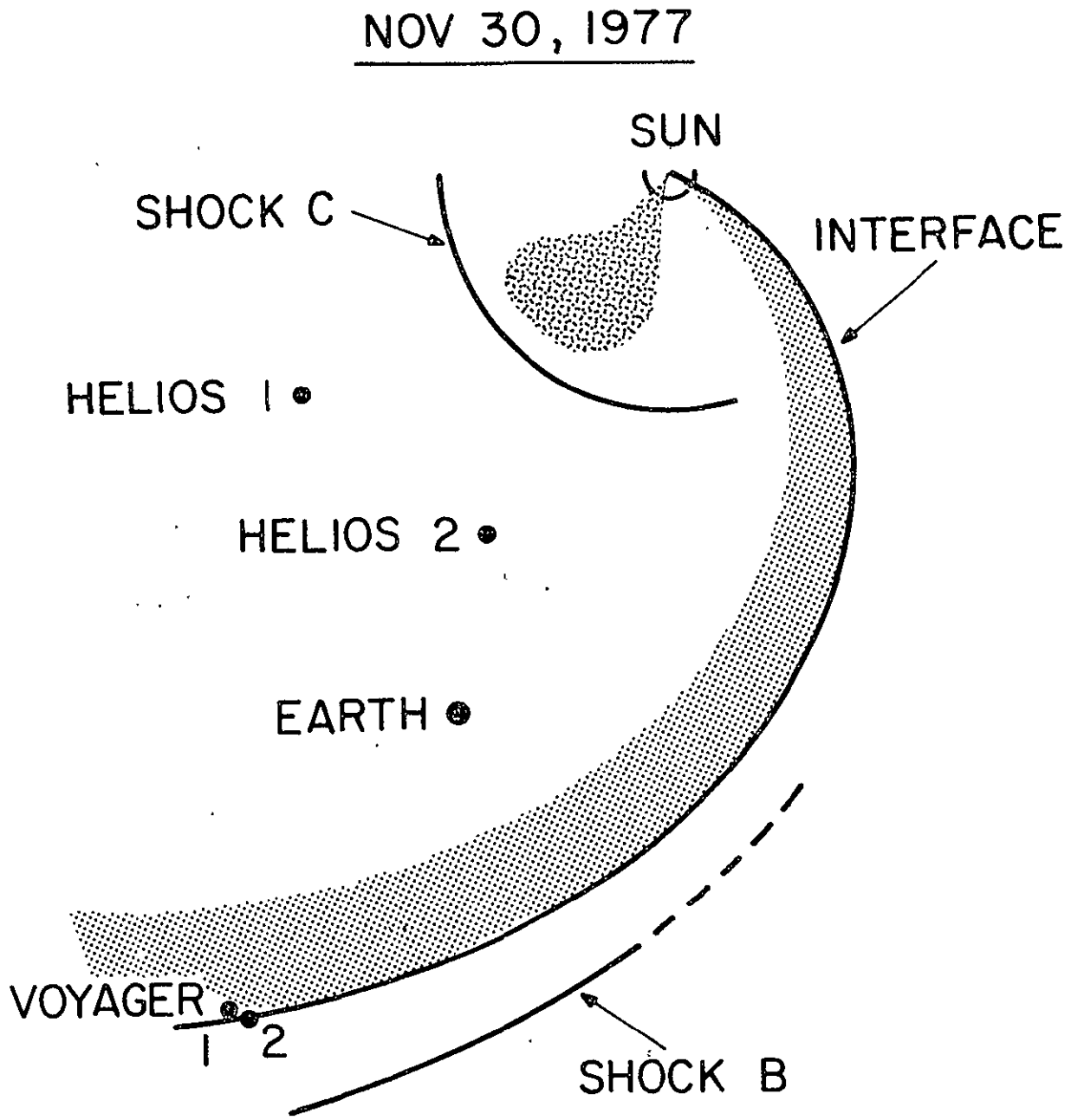
NOV 30, 1977
SUN
SHOCK C
INTERFACE
HELIOS 1
HELIOS 2
EARTH
VOYAGER
1
2
SHOCK B

Figure 15

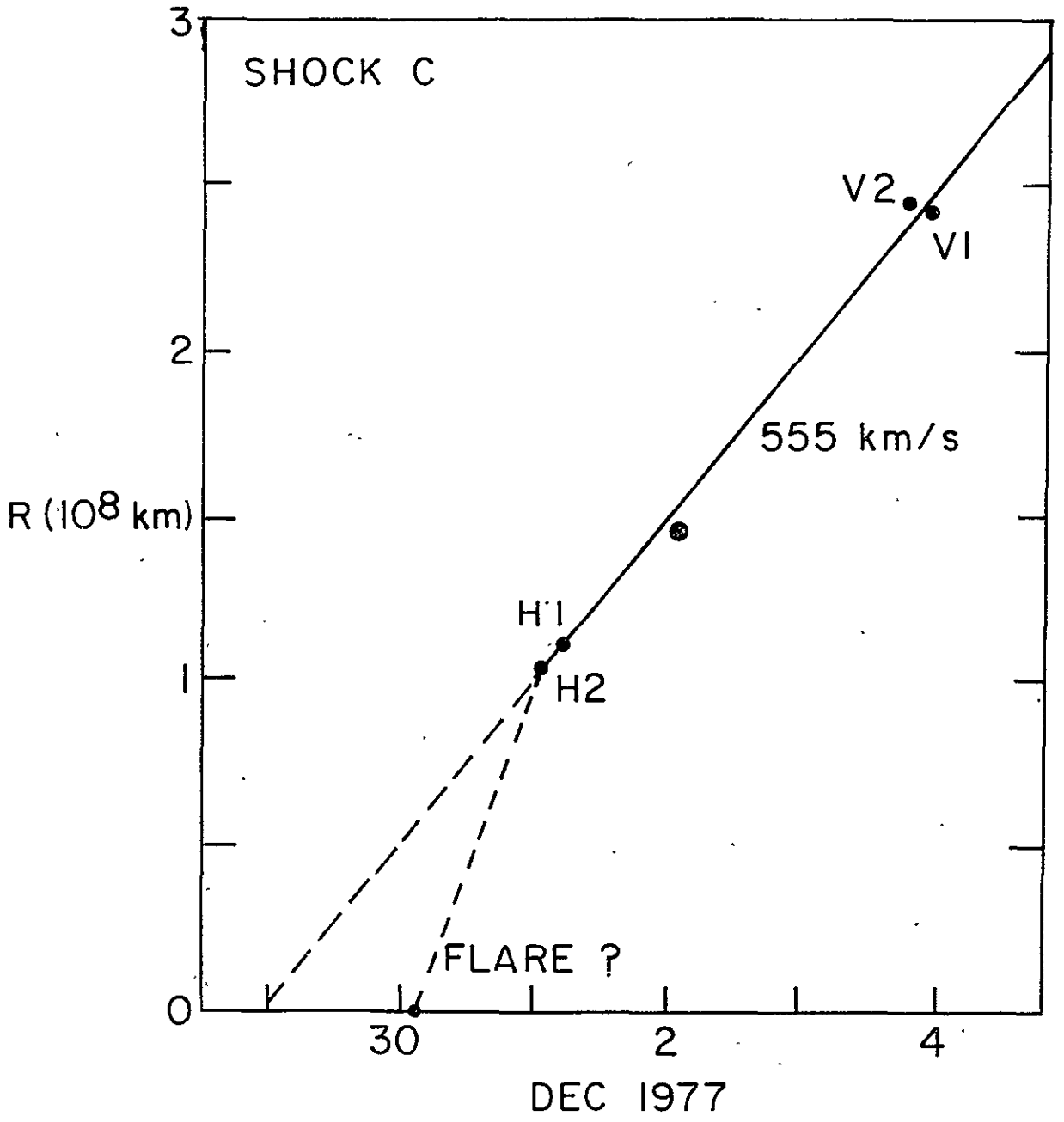

Figure 16

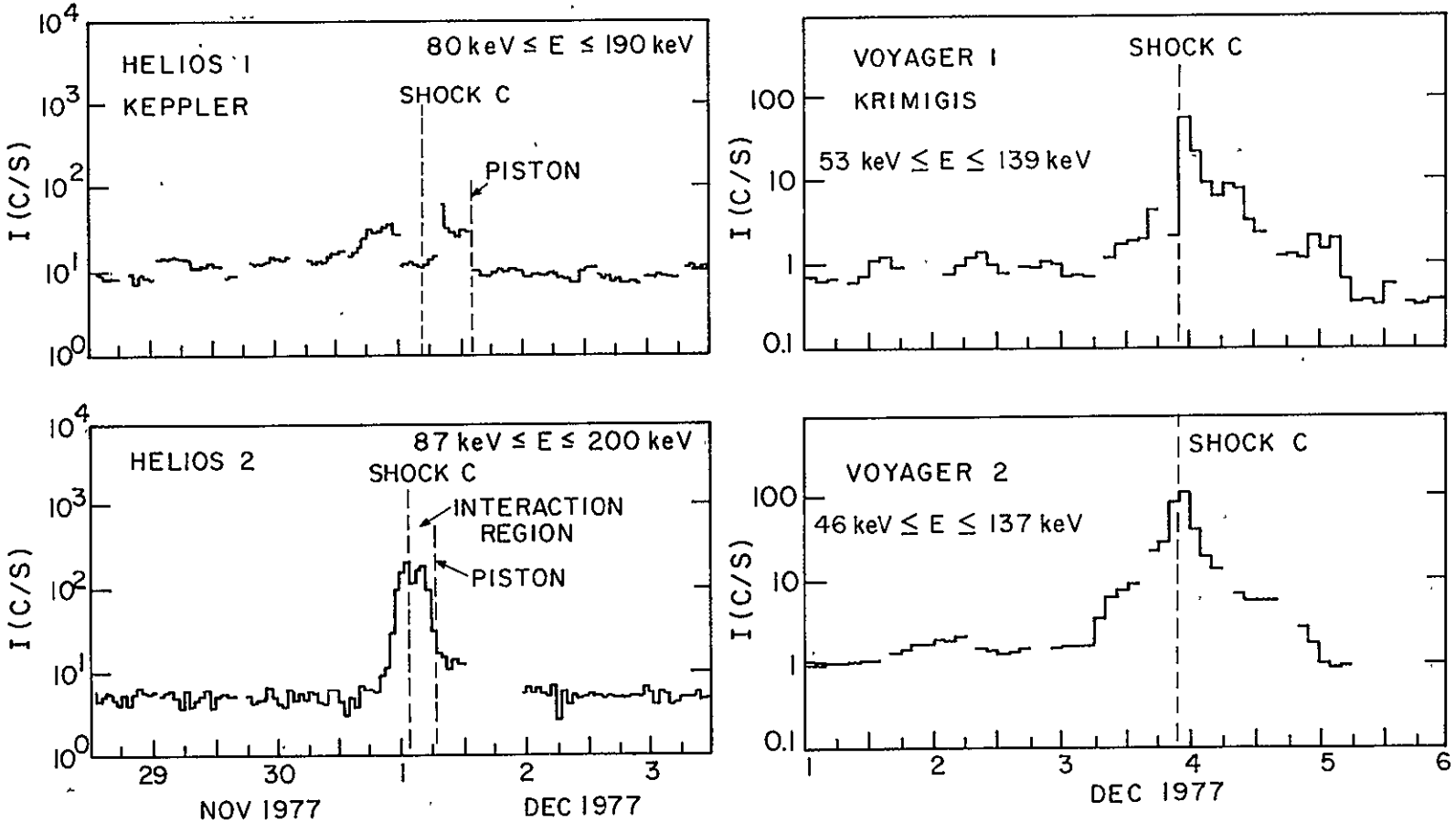
HELIOS 1
KEPPLER
80 keV ≤ E ≤ 190 keV
SHOCK C
PISTON
I (C/S)
VOYAGER 1
KRIMIGIS
53 keV ≤ E ≤ 139 keV
SHOCK C
HELIOS 2
87 keV ≤ E ≤ 200 keV
SHOCK C
INTERACTION REGION
PISTON
29
30
1
2
3
NOV 1977
DEC 1977
VOYAGER 2
46 keV ≤ E ≤ 137 keV
SHOCK C
1
2
3
4
5
6
DEC 1977

Figure 17

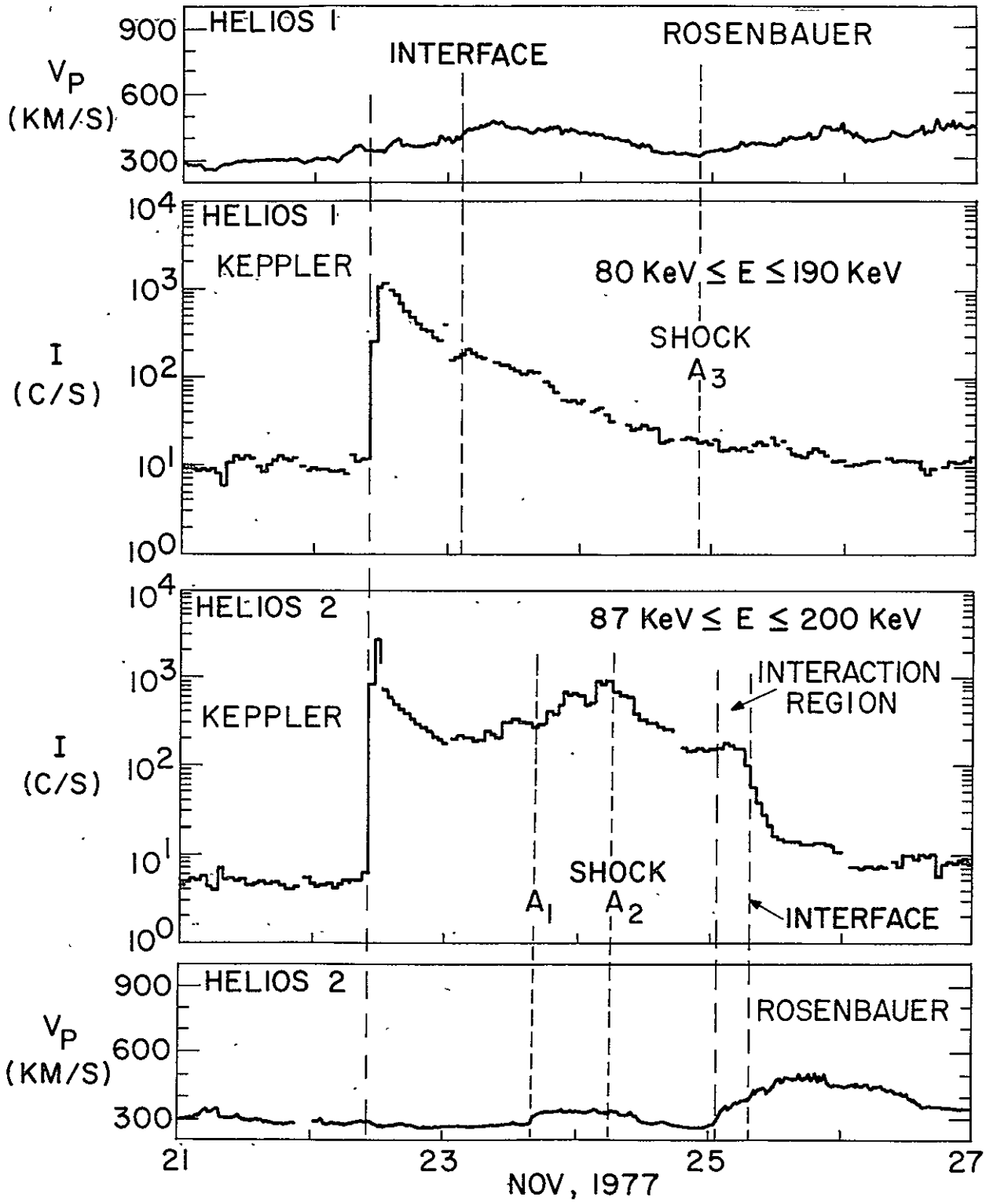
HELIOS 1
ROSENBAUER
INTERFACE
V_P (KM/S)
900
600
300
HELIOS 1
KEPPLER
80 KeV ≤ E ≤ 190 KeV
SHOCK
A_3
I (C/S)
10^4
10^3
10^2
10^1
10^0
HELIOS 2
87 KeV ≤ E ≤ 200 KeV
KEPPLER
INTERACTION REGION
SHOCK
A_1
A_2
INTERFACE
HELIOS 2
ROSENBAUER
21
23
25
27
NOV, 1977

Figure 18

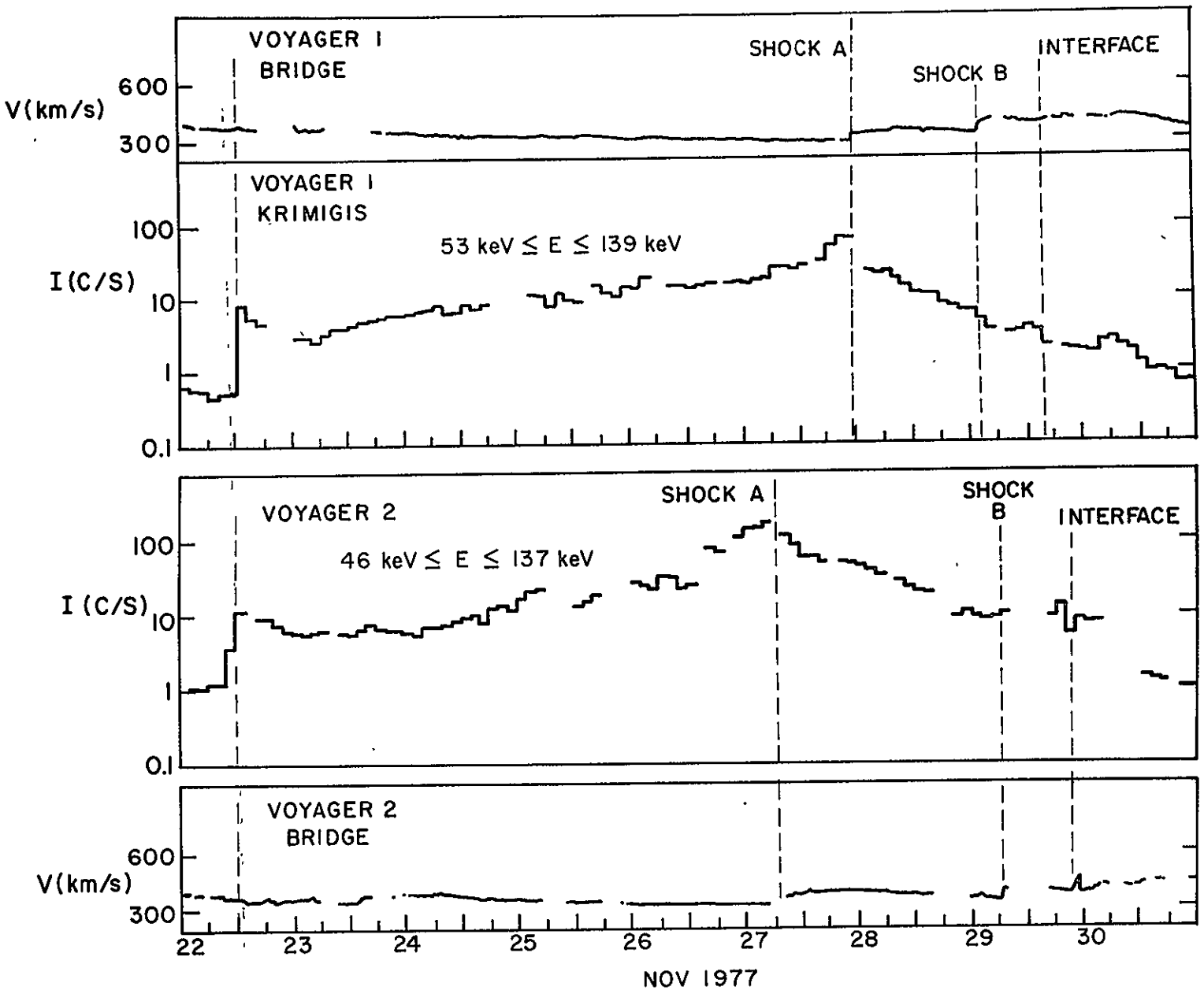
VOYAGER 1
BRIDGE
SHOCK A
SHOCK B
INTERFACE
V(km/s)
600
300
VOYAGER 1
KRIMIGIS
53 keV ≤ E ≤ 139 keV
I(C/S)
100
10
1
0.1
VOYAGER 2
SHOCK A
SHOCK B
INTERFACE
46 keV ≤ E ≤ 137 keV
I (C/S)
100
10
1
0.1
VOYAGER 2
BRIDGE
V(km/s)
600
300
22
23
24
25
26
27
28
29
30
NOV 1977

Figure 19

BIBLIOGRAPHIC DATA SHEET

1. Report No.	2. Government Accession No.	3. Recipient's Catalog No.
TM 80333		

4. Title and Subtitle	5. Report Date
Interplanetary Particles and Fields, November 22-December 6, 1977: Helios, Voyager, and IMP Observations between 0.6 AU and 1.6 AU	July 1979
	6. Performing Organization Code
7. Author(s) L. Burlaga, R. Lepping, R. Weber, T. Armstrong, C. Goodrich, J. Sullivan, D. Gurnett,	8. Performing Organization Report No.
9. Performing Organization Name and Address NASA/GSFC Laboratory for Extraterrestrial Physics Interplanetary Physics Branch, Code 692 Greenbelt, MD 20771	10. Work Unit No.
	11. Contract or Grant No.
	13. Type of Report and Period Covered Technical Memorandum
12. Sponsoring Agency Name and Address	14. Sponsoring Agency Code

15. Supplementary Notes
~~XXXXXXXXXXXXXXXX~~ #7 Cont'd.

P. Kellogg, E. Keppler, F. Mariani, F. Neubauer, H. Rosenbauer, R. Schwenn

16. Abstract

See attached.

17. Key Words (Selected by Author(s))	18. Distribution Statement
shock waves, solar wind, magnetic fields	

19. Security Classif. (of this report)	20. Security Classif. (of this page)	21. No. of Pages	22. Price*
U	U	56	

*For sale by the National Technical Information Service, Springfield, Virginia 22151.

ABSTRACT

In the period November 22 - December 6, 1977, three types of interplanetary flows were observed--a corotating stream, a flare-associated shock wave, and a piston-driven shock wave. Helios-2, IMP-7, 8, and Voyager-1, 2 were nearly radially aligned at $\lesssim$ 0.6 AU, 1 AU and 1.6 AU, respectively), while Helios-1 was at $\lesssim$ 0.6 AU and 35° E of Helios-2. The instruments on these spacecraft provided an exceptionally complete description of the particles and fields associated with the three flows and corresponding solar events. Analysis of these data revealed the following results. 1) A coronal hole associated corotating stream, observed at 0.6 AU and 1 AU, destroyed itself before it reached 1.6 AU. The stream interface corotated and persisted with little change in structure even though the stream disappeared. A forward shock was observed ahead of the interface, and moved from Helios-2 at 0.6 AU to Voyager-1, 2, at 1.6 AU; although the shock was ahead of a corotating stream and interface, the shock was not corotating, because it was not seen at Helios-1, probably because the corotating stream was not stationary. 2) An exceptionally intense type III burst was observed in association with a 2B flare of November 22. The exciter of this burst--(a beam of energetic electrons)--and plasma oscillations (presumably caused by the electron beam) were observed by Helios-2. 3) A non-spherical shock was observed in association with the November 22, flare. This shock interacted with another shock between 0.6 AU and 1 AU, and they coalesced to form a single shock that was identified at 1 AU and at 1.6 AU. 4) A shock driven by a piston was studied. In the piston, the density and temperature were usually low and the magnetic field intensity was relatively high. This region was preceded by a directional discontinuity at which the magnetic field intensity dropped appreciably. The shock appeared to move globally at a uniform speed, but locally there were fluctuations in speed and direction of up to 100 km/s and 40°, respectively. 5) Three types of electrostatic waves were observed at the shocks, in different combinations. The detailed wave profiles differed greatly among the shocks, even for spacecraft separations $\lesssim$ 0.2 AU, indicating a strong dependence on local conditions. However, the same types of fluctuations were observed at 0.6 AU and at 1.6 AU. 6) Energetic (50-200 keV) protons were accelerated by

the shocks. The intensities and durations of the fluxes varied by a factor of 12 over longitudinal distances of $\gtrsim$ 0.2 AU. The intensities were higher and the durations were lower at 1.6 AU than at 0.6 AU, suggesting a cumulative effect. 7) Energetic ($\gtrsim$ 50 keV) protons from the November 22, flare were observed by all the spacecraft. During the decay, Helios-1 observed no change in intensity when the interface moved past the spacecraft, indicating that particles were injected and moved uniformly on both sides of the interface. Helios-2 observed an increase in flux not seen by Helios-1, reaching maximum at the time that a shock arrived at Helios-2. The intensity dropped abruptly when the interface moved past Helios-2, indicating that the "extra" particles seen by Helios-2 did not penetrate the interface.